THE CRYSTAL STRUCTURE OF

ANTHRACENE AND TETRACENE.

THESIS

Presented for the degree of

Doctor of Philosophy

in the

University of Glasgow

by

Violet Catherine Sinclair, B.Sc.

August 1949.

PREFACE.

The work on tetracene described in this thesis, will, when completed, be published conjointly with Professor J. Monteath Robertson.

The first half of the experimental section of the work on anthracene (up to the point of obtaining the measured structure factors) was carried out in close collaboration with Dr. A. M. Mathieson. The completed research into the crystal structure of anthracene is being prepared for publication in conjunction with Dr. A. M. Mathieson and Professor J. Monteath Robertson.

I wish to offer my sincere thanks to Professor Robertson for suggesting the problems for research, and for his constant assistance and encouragement throughout the work. I also wish to thank Dr. E. Clar for samples of tetracene, and the Department of Scientific and Industrial Research for a Maintenance Allowance.

V. C. S.

August 1949.

The University of Glasgow.

SUMMARY.

The crystal structures of the hydrocarbons anthracene and tetracene have been investigated by X-ray diffraction methods.

In the former compound a triple Fourier analysis was carried out, and the atomic co-ordinates have been determined with great accuracy. The observed variations in bond lengths within the molecule have been discussed in terms of the resonance structures, and a measure of agreement has been found to exist between the observed and calculated values. The effect of thermal vibration and the presence of hydrogen atoms have both been clearly indicated in the Fourier contour map drawn in the plane of the molecule.

The preliminary investigation into the crystal structure of tetracene, by a double Fourier analysis, has led to a determination of the atomic parameters, and a close similarity to the anthracene structure has been revealed.

CONTENTS.

INTRODUCTION.

The structure of condensed ring aromatic hydrocarbons has attracted attention since the early days of X-ray crystallography, the earliest investigation of naphthalene and anthracene being by W.H.Bragg in 1921.

Organic chemists were of the opinion that the aromatic ring in benzene was a regular planar hexagon and it was thought likely that the polycyclic aromatic hydrocarbons would show this same regularity of structure.

The first detailed measurements of bond distances in these compounds were made by Robertson (1933), and the results indicated that the molecules of naphthalene and anthracene were planar and consisted of regular hexagons, the distance between atomic centres being 1.41A.

In recent years theoretical chemists have been turning their attentions more and more to the question of variations in the bond distances in aromatic hydrocarbons, and so many mathematical treatments of these variations have been given, that it is of some importance that experimental results should be obtained, which are accurate enough to admit of comparison with the theoretically derived values.

The first experimental demonstration of this

deviation from complete regularity was given in the case of coronene by Robertson and White (1945). Here, due to the symmetry of the compound, the values of the bond lengths are mean values of several identical bonds, and so the accuracy is greatly increased. However, two dimensional determinations of structure, except in special cases of this nature, possess sufficient inaccuracy, in the co-ordinates of unresolved atoms, largely to vitiate small variations apparent in bond lengths. In most cases these are of the same order as the experimental error.

The simpler hydrocarbons are most amenable to rigid mathematical treatment and for this reason it was decided to elucidate fully the structures of anthracene and naphthalene by X-ray diffraction methods.

Since the previous structural determination of anthracene had been taken almost to the limit of the double Fourier method it was unlikely that any further refinement of the co-ordinates could be obtained by the same means, owing to the large amount of overlapping in the projections. Thus it was considered necessary to undertake a full three dimensional determination of the structure, which by reason of its greater accuracy and complete resolution of each atom should provide very exact atomic co-ordinates and bond lengths.

The precise limits of inaccuracy in this method have been determined theoretically by Booth (1946). All the

possible sources of error encountered in a three dimensional Fourier synthesis have been listed and maximum values determined for each. The experimental error in this treatment is almost negligible and is quoted as 0.003A for a carbon atom.

A larger source of error however is that due to non-infinite limits of summation of the Fourier series. The theoretical determination of this error for polyatomic structures is hardly possible, but for a diatomic structure the upper limit of the discrepancy is 0.02A. It is possible to determine the error experimentally by carrying out an additional synthesis using the calculated values of the structure factors instead of the observed values. The deviations in the resulting maxima from the original positions give the errors in the atomic co-ordinates. This was done in the case of geranylamine hydrochloride, Jeffrey (1945), and the deviations were found to be of the same order as predicted (0.02A).

Anthracene being purely a hydrocarbon gives a more convergent series than geranylamine hydrochloride and the error from this source should therefore be correspondingly less. Thus it seems probable that variations in carbon-carbon bond lengths which are in the region of 0.01A to 0.05A should be definitely determinable by the method of three dimensional Fourier synthesis.

Another closely related problem was the determination of the crystal structure of tetracene by X-ray diffraction methods. This hydrocarbon is the next member of the homologous series starting with naphthalene and anthracene, and by reason of its extended four ring system gives rise to a greater number of resonance forms (Pauling and Wheland 1933). Thus the variations in bond lengths in tetracene will be greater than in the two preceding hydrocarbons.

It has been shown that in favourable cases the variations in bond lengths in polycyclic aromatic hydrocarbons can be discerned in a two dimensional structure determination (Robertson and White, 1945; 1947; White 1948), and it was hoped that in tetracene these variations would be large enough to be similarly observed.

A noticeable feature of this compound is that it belongs to the triclinic system unlike the two preceding hydrocarbons, which are both monoclinic. It is therefore of interest to make a comparison of the crystal structure of tetracene with those of naphthalene and anthracene, which bear a very close resemblance to each other.

The unit cell dimensions had previously been measured by Hertel and Bergk (1936), but no attempt was

made to determine the space group or the atomic co-ordinates.

It was therefore with the aim of elucidating the crystal structure to the limit of the double Fourier method that the present study was undertaken.

THE CRYSTAL STRUCTURE OF ANTHRACENE.

Crystal Data.

Anthracene $C_{14}H_{10}$; molecular weight 178.2; melting point 218°C; monoclinic prismatic. Lengths of axes:- a=8.561A, b=6.036A, c=11.163A, β=124°42' Space group $P2_{1/a}$. Two molecules per unit cell. Molecular symmetry - centre. Molecular volume, 474.22A^3. Absorption co-efficient for X-rays (λ=1.54A), μ=6.54 per cm. Total number of electrons per unit cell=$F_{(000)}$=188.

Experimental.

Crystals were grown by slow formation during two or three days from pure amyl acetate, using a vacuum flask to ensure very gradual cooling of the solution. This produced mainly clear shining needle-shaped crystals, elongated in the direction of the b-axis. A number of more evenly developed specimens were also obtained by this method, the (001) face showing major development, and these were more suitable for intensity determinations.

Recording of hkl reflections.

The method employed to record the X-ray reflections was to explore all the possible layer lines associated with each axis by means of an equi-inclination Weissenberg camera

using Cu K_α radiation (λ=1.54A). The camera employed was built in the workshop in this department, and is a modification of J.M.Robertson's two crystal spectrometer. The whole spectrometer, with a solid metal base, is laid on metal to achieve smooth movement, and rotates about an axis which coincides with the crystal. The film carrier is semi-circular and thus is easily removed and loaded.

Since the direct X-ray beam and the reflected beam are inclined at the same angle to the rotation axis, the reflected beam passes through the intersect of the rotation axis and the reciprocal lattice layer. The origin of the reciprocal lattice layer or a point on one of the reciprocal lattice rows then coincides with this point (for all but triclinic cases). This greatly simplifies the identification of reflections and avoids the application of graphical constructions necessary in the normal beam method.

A further advantage of the equi-inclination Weissenberg is that the range of n layers is greater than for the normal beam method, since the range of angle of direct to reflected beam is here 120° as compared with 90° for the normal beam method. The physical dimensions of the X-ray tube and camera, however, reduce the maximum equi-inclination angle in this case to a value of 28°.

Table I.

Zones obtained and crystal dimensions in millimetres.

b axis		a axis		c axis		101 diagonal	
h0l)		0kl)		hk0)		$hk\bar{h}$)	
)	.37	)	.47	)	.18	)	.39
h1l)		1kl)		hk1)		$hk\bar{h}-1$)	
)	x	)	x	)	x	)	x
h2l)		2kl)		hk2)		$hk\bar{h}-2$)	
)	.66	)	.68	)	.44	)	.47
h3l)		3kl)		hk3)		$hk\bar{h}-3$)	
)	x	)	x	)	x	)	x
		4kl)		hk4)		hkh-4)	
	.68		.79	)	.47	)	.75
				hk5)		$hk\bar{h}-5$)	

Exploring the layer lines associated with the three principal crystal axes to the limit of the equi-inclination camera, gave four series on the b axis, five on the a axis, and six on the c axis, but it was apparent from examination of the reciprocal lattice that a large number of reflections from (hkl) planes would not appear on any of these films. Another axis of rotation had, therefore, to be chosen to include these planes, and the most suitable was the [101] axis of which the zero layer yields the ($hk\bar{h}$) planes, and the indices of the general n layer are ($hk\bar{h}-n$). This choice of axis gives practically all the remaining reflections. The zones obtained together with the dimensions of the crystals employed were as shown in Table I.

Estimation of Intensities.

To correlate very strong and very weak reflections the multiple film technique (Robertson 1943) was employed.

Four, or at most, five films are loaded together, being separated by two thicknesses of black paper, and if submitted throughout to exactly similar conditions the recorded intensities will be strictly comparable. To increase the range of intensities obtained, two series were recorded for most of the zones, having time exposures in the ratio of sixteen to one.

Previous measurements on Ilford film had determined exactly the film to film ratio, but as Kodak films were used throughout this investigation, it was necessary to determine the ratio for this type, since it differs from that of Ilford. Two methods were used -

In the first the same zone of reflection was recorded on both Ilford and Kodak films, and these were compared. The ratio for Ilford being known, the best ratio for Kodak was chosen to bring the intensities to the same scale. By this method 3.0 - 3.2 was selected as the best value.

By the second method one layer of a rotation axis was isolated by the screens of the Weissenberg camera and this layer was recorded on the same pack of film for different definite times. The value obtained by this means was higher, being 3.4.

An independent check on this ratio has been made by the Kodak laboratories. The figure given is 35.5%

absorption for one film, expressing the absorbed beam as a percentage of the direct beam. It is known that two sheets of black paper decrease this by 10%. Therefore the film to film ratio by this method is 3.1 . This value is probably the most accurate as the work was carried out using a photometer and monochromatic radiation.

The intensities of the reflections on the moving film series were estimated visually. Reflections of low intensity can be compared most accurately, and since the film to film ratio was 3.1, most estimations were made in the region of one to three on the first and successive films. This simple treatment was complicated however by the larger areas and unsymmetrical shapes of the stronger reflections and it was found that the personal factor was greater in compensating for this; but as these reflections also occurred in other zones with more moderate intensities the error involved was not appreciable.

For the higher layers the X-ray beam is striking the film obliquely, and the film to film ratio must be modified accordingly. This was done approximately by multiplying the factor by $1/\cos\mu$. For the (h2l) series this gave a value of 3.2 and for the (h3l) a value of 3.4.

The maximum range of intensities observed was five thousand to one in the (hol) zone, but a range of one thousand to one was general. 690 planes out of a possible

1085 were observed. These intensity determinations were carried out independently by two research students and were found to agree within 10% of each other.

Corrections Applied.

The observed intensities were corrected by the usual Lorenz and polarisation factors, and in view of the accuracy required, it was thought advisable to apply an absorption correction despite the relatively weak absorption of X-rays by anthracene (6.54 per centimetre). To make an accurate estimate of absorption would be extremely tedious and accordingly one estimate was made for each plane of the path through the centre of the crystal projection. This can be done graphically by calculating the angle of incidence and reflection for each plane, but a more rapid method was evolved utilising a scale drawing of the crystal section, the reciprocal lattice and the property of the reflecting circle. The values of the path of the X-ray beam through the crystal derived in this way, were then substituted in the equation

$$I=I_o e^{-\mu t}$$

where I was the observed intensity, t the mean path through the crystal, and μ the co-efficient of absorption. The value of $e^{-\mu t}$ varied between 1.27 and 1.62.

For n layer reflections a further correction had to be applied, since these planes which lie at an angle to

the axis rotate more slowly than planes in the zero layer (Cox and Shaw 1930). This correction has been evaluated for equi-inclination cameras by G.Tunell (1939), and is given by

$$D_e = \frac{\cos^2\mu - \cos^2\theta}{\sin\theta}$$

where μ is the equi-inclination angle, and θ is the Bragg reflection angle.

Correlation of Relative Structure Factors.

The values for the (hol) zone given by Robertson (1933) which were measured in absolute units with the ionisation spectrometer and Robinson's photometer, were utilised to place the (hol) zone reflections on the absolute scale.

From these reflections the(hll) zone was placed on the absolute scale, using the (2kl), (hk$\bar{h}$-1), (hk$\bar{h}$-2), (hk$\bar{h}$-3), (hk$\bar{h}$-4), (hk$\bar{h}$-5) zones as intermediaries, since they contained a large number of planes common to both zones. The (h2l) and (h3l) zones were placed on the absolute scale in a similar manner, and it was then a relatively simple matter to correlate all the other zones. The general method employed is illustrated in Table II.

The mean of the various values given by the different zones was taken as being the true structure factor, except in the case of strong planes where extinction effects

are more important. In this case the highest value was usually accepted.

Table II.

Correlation of measured structure factors.

hol absolute	(2kl) (hkh-1) (hkh-2) (hkh-3) (hkh-4) (hkh-5) approx. absolute	hll absolute	(2kl) (hkh-1) (hkh-2) (hkh-3) (hkh-4) (hkh-5) absolute	h2l h3l absolute

Constancy of Discrepancy.

The discrepancy between the values of planes observed in different zones was calculated from the formula

$$\Delta = \frac{\sum \left| |F'obs| - |F''obs| \right|}{\sum |F'obs|}$$

where F'obs is the value from one zone and F"obs the value from another zone. This discrepancy was found always to be in the region of 10%.

Two Dimensional Fourier Analysis.

The new experimental results increased the number of observed planes in the (hol) zone to a total of 65 compared with the previous total of 35 (Robertson 1933). In view of this extended range it was thought advisable to

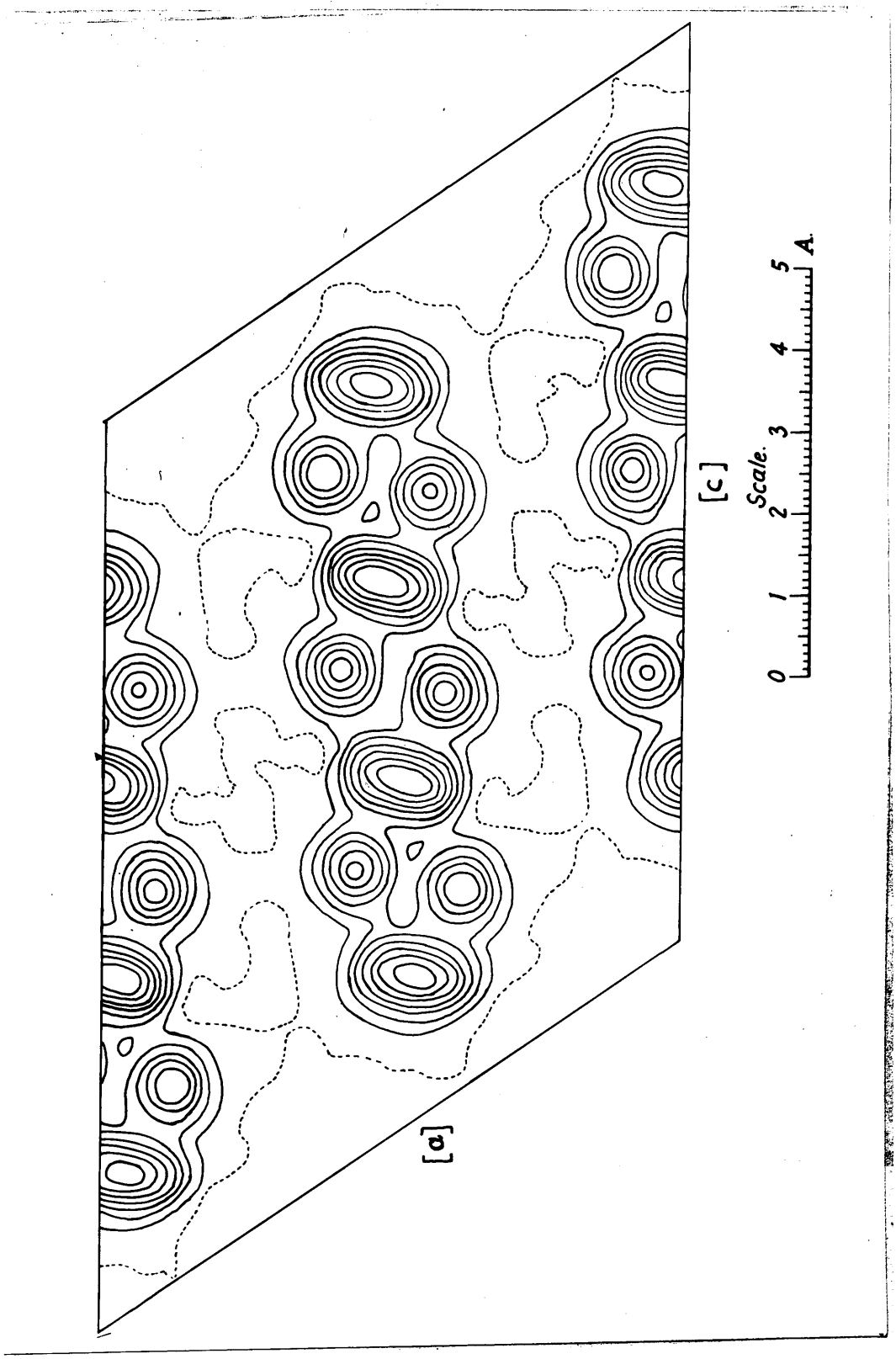

Fig. 1. Normal projection of the unit cell along the b crystal axis. Each contour line represents a density increment of one electron per A^2, the one electron line being dotted.

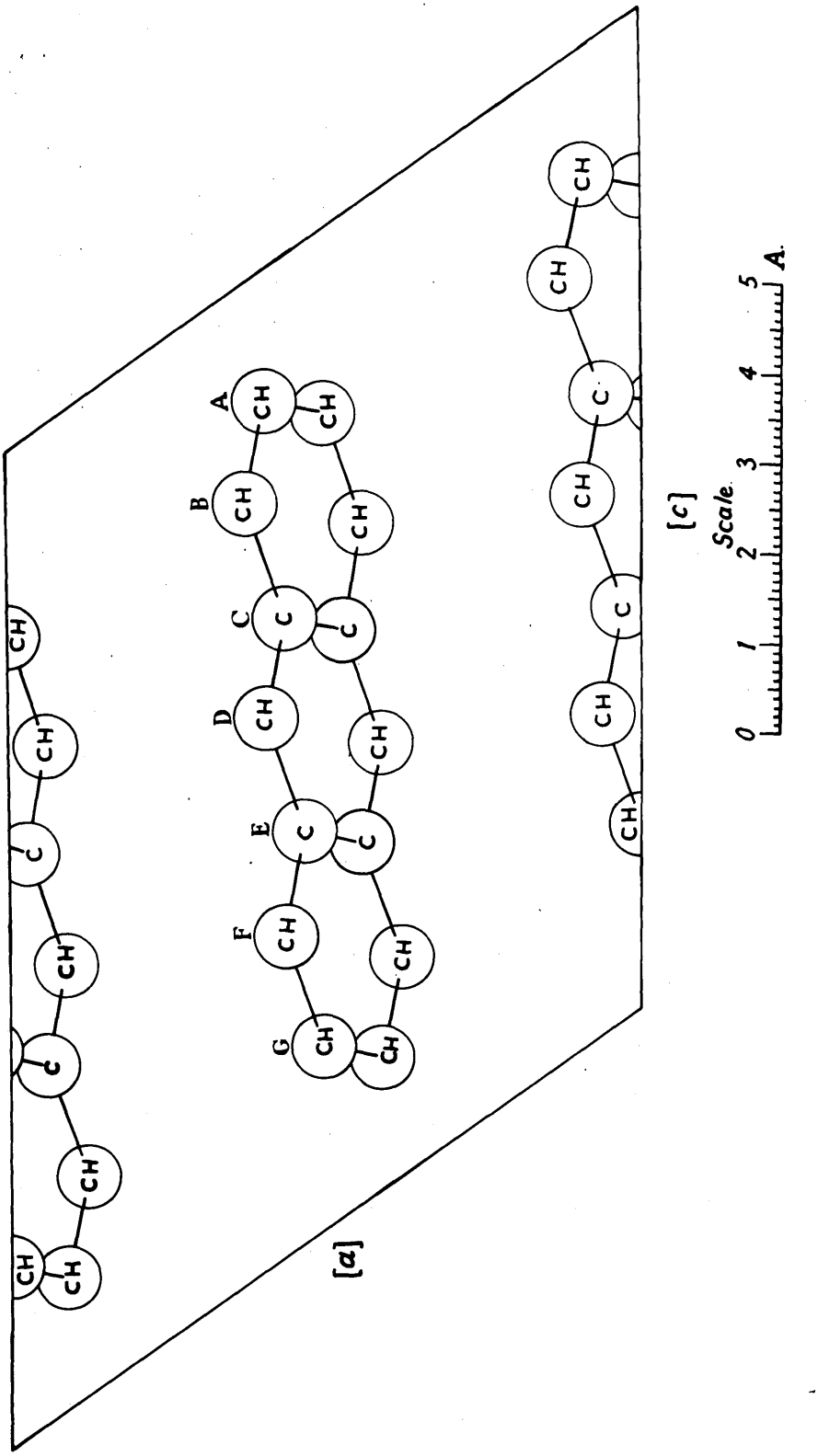

Fig. 2. Arrangement of the molecules in the b axis projection.

repeat the two dimensional Fourier synthesis introducing the extra observed planes.

The density of scattering matter per unit area for projection along the b axis is given by

$$\rho(x,z) = \frac{1}{A}\sum_{-\infty}^{+\infty}\sum_{-\infty}^{+\infty} F_{..} \cos 2\pi\left(\frac{hx}{a} + \frac{lz}{c}\right)$$

$$\rho(x,z) = \frac{1}{A}\sum_{-\infty}^{+\infty}\sum_{-\infty}^{+\infty} F(hol)\cos 2\pi\left(\frac{hx}{a} + \frac{lz}{c}\right)$$

into 30 and 60 parts, the divisions being .286A and .186A respectively. Only one quarter of the cell required to be determined, as the remainder is reproduced by the symmetry elements.

Fig. 1. shows the distribution of scattering matter for the (hol) projection. The molecules are separated, three of the atoms of the asymmetric unit being clearly defined, and showing a high degree of spherical symmetry. Certain improvements in contour disposition are shown in this Fourier map compared with previous results.

The new co-ordinates obtained from this Fourier analysis, taking the centre of symmetry as origin are given in Table III. These do not differ greatly from the values given by Robertson (1933).

Table III.

	xA	zA		xA	zA
c_1	0.79	4.10	c_5	0.24	-0.95
c_2	1.07	3.14	c_6	0.51	-1.99
c_3	0.52	1.54	c_7	0.00	-3.53
c_4	0.77	0.57			

Calculation of (hkl) Geometrical Structure Factors.

Since the projections looking down on the a and c axes give very poor resolution, and since the new x and z co-ordinates did not show great deviation from the previous values, it was decided not to repeat these projections, but to accept Robertson's value for the y co-ordinates in calculating the (hkl) structure factors.

For the space group $P_{2_1/a}$ the geometrical structure factor has the form

$$S = 4\cos 2\pi\left(\frac{hx}{a} + \frac{lz}{c} + \frac{bh+ak}{4ab}\right)\cos 2\pi\left(\frac{ky}{b} - \frac{bh+ak}{4ab}\right) \quad -- (1).$$

which may be rewritten in the form

$$S = 4\cos 2\pi\left(\frac{hx}{a} + \frac{lz}{c}\right)\cos 2\pi\left(\frac{ky}{b}\right) \quad \text{for } h+k = 2n \quad ----(2).$$

and

$$S = -4\sin 2\pi\left(\frac{hx}{a} + \frac{lz}{c}\right)\sin 2\pi\left(\frac{ky}{b}\right) \quad \text{for } h+k = 2n+1 \quad ---(3).$$

To simplify these calculations all the angles of the form $h\theta_1 \pm l\theta_3$ were calculated (where $\theta_1 = 2\pi x/a$, $\theta_2 = 2\pi y/b$, $\theta_3 = 2\pi z/c$), and the corresponding sines and cosines of these angles obtained for each atom. Similarly the sines and cosines of all the angles $k\theta_2$ were determined. It was thus possible to determine the 1085 geometrical structure factors by substitution in (2) and (3) and summing over the 7 atoms

for each plane. The maximum possible value for S when $\theta_1 = \theta_2 = \theta_3 = 0$ is 7 and the maximum value actually found was S = 5.68.

The Atomic Scattering Curve.

It was decided to use the original scattering curve as derived by Robertson for anthracene, although it had been apparent from the new (hol) projection that it should fall off more sharply as 2sinθ approaches 2, and rise more sharply as 2sinθ approaches zero. This, however, in no way affects the phases but merely alters the magnitude of the calculated structure amplitudes. These were obtained from the relation

$$F = S \times f_c \times \frac{F_{(000)}}{100} \times \frac{1}{7}$$

where $S_{max} = 7$, and $f_{c\ max} = 100$.

Preparation for Computation.

For the purposes of computation these structure amplitudes F were converted to F' by the relation

$$F'_{(hkl)} = F_{(hkl)} \times \frac{1000}{\text{vol. of unit cell.}}$$

Thus the final electron density figures were calculated on the basis of 1 electron per cubic A = 1000 which may be compared with the usual value of 1 electron = 100 used in two dimensional work. A higher standard of accuracy was therefore possible in selecting the atomic

centres.

Since a structure factor with wrong sign attached introduces twice the error caused by omitting it completely, it was considered advisable to omit all the structure factors of doubtful phase. This was done by inserting only structure amplitudes which had a geometrical structure factor $>$ .15 (max. = 7.0).

These omissions reduced the number of planes included in the computation from 690 to 667, which is 61.5% of the total number of planes within the sphere of reflection for Cu K_α radiation.

Numerical Evaluation of the Triple Fourier Series.

To evaluate a full triple Fourier series using the devices applicable to double Fourier series would involve a large amount of purely mechanical labour. In view of this fact the summation was carried out on a Hollerith International Business Machine by the Scientific Computing service, London. This machine utilised a punched card system in which the positions of the punched holes correspond to the magnitude and phase of the Fourier term (Booth 1948).

Each unit cell edge was divided into sixty parts (giving an interval of 0.1427A for the a axis, 0.1006A for the b axis, and 0.1861A for the c axis). The electron density was summed over one complete asymmetric unit, in which x had the values 0 to 30/60ths, y from 0 to 30/60ths

and z from 0 to 60/60ths. The electron density at the point (x,y,z) is given by

$$\rho(x,y,z) = \frac{1}{V}\sum_{-\infty}^{+\infty}\sum_{-\infty}^{+\infty}\sum_{-\infty}^{+\infty}\left|F(hkl)\right| \cos 2\pi\left(\frac{hx}{a} + \frac{ky}{b} + \frac{lz}{c}\right)$$

This may be reduced to

$$\rho(x,y,z) = \frac{4}{V}\sum_{0}^{+\infty}\sum_{0}^{+\infty}\sum_{0}^{+\infty}\Bigg\{\left[F(hkl) + F(hk\bar{l})\right]\cos 2\pi\frac{hx}{a}.\cos 2\pi\frac{ky}{b}.\cos 2\pi\frac{lz}{c}$$

$$+\left[F(hk\bar{l}) - F(hkl)\right]\sin 2\pi\frac{hx}{a}.\sin 2\pi\frac{ky}{b}.\sin 2\pi\frac{lz}{c}$$

for h+k even

$$-\left[F(hkl) + F(hk\bar{l})\right]\sin 2\pi\frac{hx}{a}.\sin 2\pi\frac{ky}{b}.\sin 2\pi\frac{lz}{c}$$

$$+\left[F(hk\bar{l}) - F(hkl)\right]\cos 2\pi\frac{hx}{a}.\cos 2\pi\frac{ky}{b}.\cos 2\pi\frac{lz}{c}\Bigg\}$$

for h+k odd.

which is the form most suitable for use in the Hollerith machine. The sums and differences of the structure factors for l positive and negative which have to be introduced into this expression are then obtained from a consideration of the multiplicities of the various terms.

These are as follows

F(hkl)	4	if $F(hk\bar{l})$ is given.
F(okl)	4	if $F(ok\bar{l})$ is not given.
F(hko)	4	
F(hol)	2	if $F(ho\bar{l})$ is given.
F(oko)	2	
F(ool)	2	if $F(oo\bar{l})$ is not given.
F(hoo)	2	
F(ooo)	1	

and hence for all values of l the following sums may be formed

	h even	h odd
for k = 0	$2\left[F(hol) + F(ho\bar{l})\right]$	
	$2\left[F(ho\bar{l}) - F(hol)\right]$	
for k > 0 and even	$4\left[F(hkl) + F(hk\bar{l})\right]$	$-4\left[F(hkl) + F(hk\bar{l})\right]$
	$4\left[F(hk\bar{l}) - F(hkl)\right]$	$4\left[F(hk\bar{l}) - F(hkl)\right]$
	$2\left[F(oko)\right]$	
for k > 0 and odd	$-4\left[F(hkl) + F(hk\bar{l})\right]$	$4\left[F(hkl) + F(hk\bar{l})\right]$
	$4\left[F(hk\bar{l}) - F(hkl)\right]$	$4\left[F(hk\bar{l}) - F(hkl)\right]$

In this way the experimental set of structure factors could be combined among themselves to give a new set of factors F' . These terms are then recorded on sheets from which the first set of cards are punched. These cards contain the magnitude and sign of the F' term together with

its appropriate(hkl) index. The cards are then passed through the tabulator combined with a set of detail cards, and the function $\sum h \begin{Bmatrix}\cos\\ \sin\end{Bmatrix} 2\pi\frac{hx}{a}$ is recorded for the given range of x. These values are then copied on to a new set of cards and the same procedure is followed in summing over y and z.

The results of this complete evaluation of the triple Fourier series was to give the electron density at 54,000 points in the asymmetric unit. These values were presented in the form of 264 sheets each containing 297 points at which the electron density had been summed.

Accurate Determination of Crystal Constants.

Before attempting a graphical interpretation of these results it was essential that the lengths of the unit cell edges and the magnitude of the β angle should be accurately known, since small deviations here would affect the measured bond distances.

It was decided that the most accurate method would be by powder photographs taken with a camera of large radius. This would give a large number of powder lines in the most accurate region ($2\sin\theta > 1$) which could be identified by means of their intensities and $2\sin\theta$ values. The intention was to use only those reflections which gave α_1, α_2 doublets, since the wavelengths of copper $K\alpha_1$, and $K\alpha_2$ radiations are very accurately known. In this way a large number of equations

of the type

$$a^2 + b^2 + c^2 + 2ac.\cos\beta = (2\sin\theta)^2$$

would be obtained, of which the $2\sin\theta$ value would be extremely accurate, and thus by solving these equations very accurate values would be obtained for a, b, c, and β.

The camera was calibrated with quartz and sodium chloride from values given by Wilson and Lipson (1941) for quartz, and those given by Bradley and Jay (1932) for sodium chloride.

A number of powder photographs of anthracene were taken but were found to be quite unsuitable for the purpose intended. The difficulties were threefold -

1. Owing to the fact that the function f_c approaches zero rapidly as $2\sin\theta$ approaches 2, no lines were obtained in the α_1, α_2 separation region of the photograph. This meant that the very accurate values for the wavelengths as determined by Seigbahn (1931) could not be used.

2. The reflections given by planes of smaller $2\sin\theta$ value were rather diffuse due to thermal agitation. This made precise measurement somewhat difficult.

3. The lines obtained could not easily be identified because it was found that in most cases about twelve planes had $2\sin\theta$ values which approximated to the measured value to 0.05 centimetre. The intensities of all these planes

would therefore be contributing to the observed line and make its measurement totally inaccurate.

In view of all these difficulties the powder method was abandoned and the axes were measured from Weissenberg moving film photographs calibrated with quartz. This was carried out by taking a Weissenberg moving film photograph of anthracene and then replacing the anthracene crystal by a thin glass fibre coated with powdered quartz. Strips of the X-ray diffracted spectra from the quartz were then printed on each side of the film.

The centres of the powder lines were accurately determined and fine lines were scored across the film joining these centres. This method was used in preference to that of printing the powder photograph right across the film in order to keep down the background, and also to eliminate the thickness of the powder lines. Thus the film was accurately calibrated for $2\sin\theta$ values.

As only a few spectra coincided with the powder lines, a method had to be evolved of accurately measuring the increment in $2\sin\theta$. This was done by graphing the $2\sin\theta$ values of the powder lines against the distances in centimetres measured by a cathetometer.

The distance of a reflection from the nearest powder line was measured on the cathetometer and by reference

to the graph the 2sinθ value of the reflection was determined. By measuring the 2sinθ values of the axial reflections and also some general (hkl) spectra, accurate values were obtained for the three axes and β. A comparison with the previous values is given in Table IV.

Table IV.

	New Values	Previous Values
a	8.561 ± 0.010A	8.58A
b	6.036 ± 0.010A	6.02A
c	11.163 ± 0.010A	11.18A
β	124° 42' ± 4'	125°

Graphical Interpretation of the Electron Density Values.

The fact that the electron density had been summed at so many points in the unit cell, necessitated the drawing of a very large number of sections. These were taken parallel to the a axis throughout the asymmetric unit, for all points which had a density greater than 0.5 electrons per cubic Angstrom unit. A noticeable feature at this stage was the uniformity of the general background which rarely exceeded 0.5 electrons per cubic Angstrom unit, and showed only occasional areas of negative density.

From these sections the electron density distribution on planes passing near the atomic centres could be drawn.

Eight such cross sections were drawn for each atom, four sections parallel to (010), and four parallel to (001).

The centre of each of the atomic cross sections was then estimated visually, and the mean of the four values taken for each set. The co-ordinates were obtained in terms of the nearest cell division so that only a very small direct measurement required to be made. (Table V).

Recalculation of the Geometrical Structure Factors.

From the refined co-ordinates a new set of geometrical structure factors was calculated. The accuracy of the previous structure determination was confirmed by the fact that only four of the planes inserted in the three dimensional Fourier synthesis had changed sign. These were all planes of small amplitude, and the error caused by inserting them would not be large.

Scattering Curve.

A new empirical scattering curve (temperature corrected) was derived by dividing the observed structure amplitude by the geometrical structure factor and plotting the atomic scattering factor so obtained against the appropriate $\sin\theta$ for the plane. Only planes having a geometrical structure factor greater than 1.5 (max. 7) were used in defining this graph.

A smooth curve was then drawn to pass through the best mean position of the points.

A table denoting the curve obtained is shown below.

$\sin\theta$ (λ=1.54) =	0.00	0.10	0.20	0.30	0.40	0.50
f_c =	100	86.6	65.8	49.3	36.4	25.5

$\sin\theta$ =	0.60	0.70	0.80	0.90	1.00
f_c =	18.4	13.1	9.7	7.3	5.9

Using this scattering curve to recalculate the structure factors, a closer agreement with the measured values was obtained. The discrepancy calculated for all the planes from the relation

$$\Delta = \frac{\sum \left| |F_{obs}| - |F_{calc}| \right|}{\sum |F_{obs}|}$$

was 19.6% and based on $F_{calc.}$ was 18.2%. The values of the observed and calculated structure factors are listed in Table XI.

Co-ordinates and Dimensions.

The sections drawn through each atom nearest the atomic centre are shown in Figs. 3-9. The shape of the electron contour is almost circular and this offers some confirmation of the belief that an atom in space is spherical. There is, however, some slight distortion due to the effect of neighbouring atoms, and comparing the diagrams at different levels near the atomic centre showed that the atoms were far from being perfect spheres.

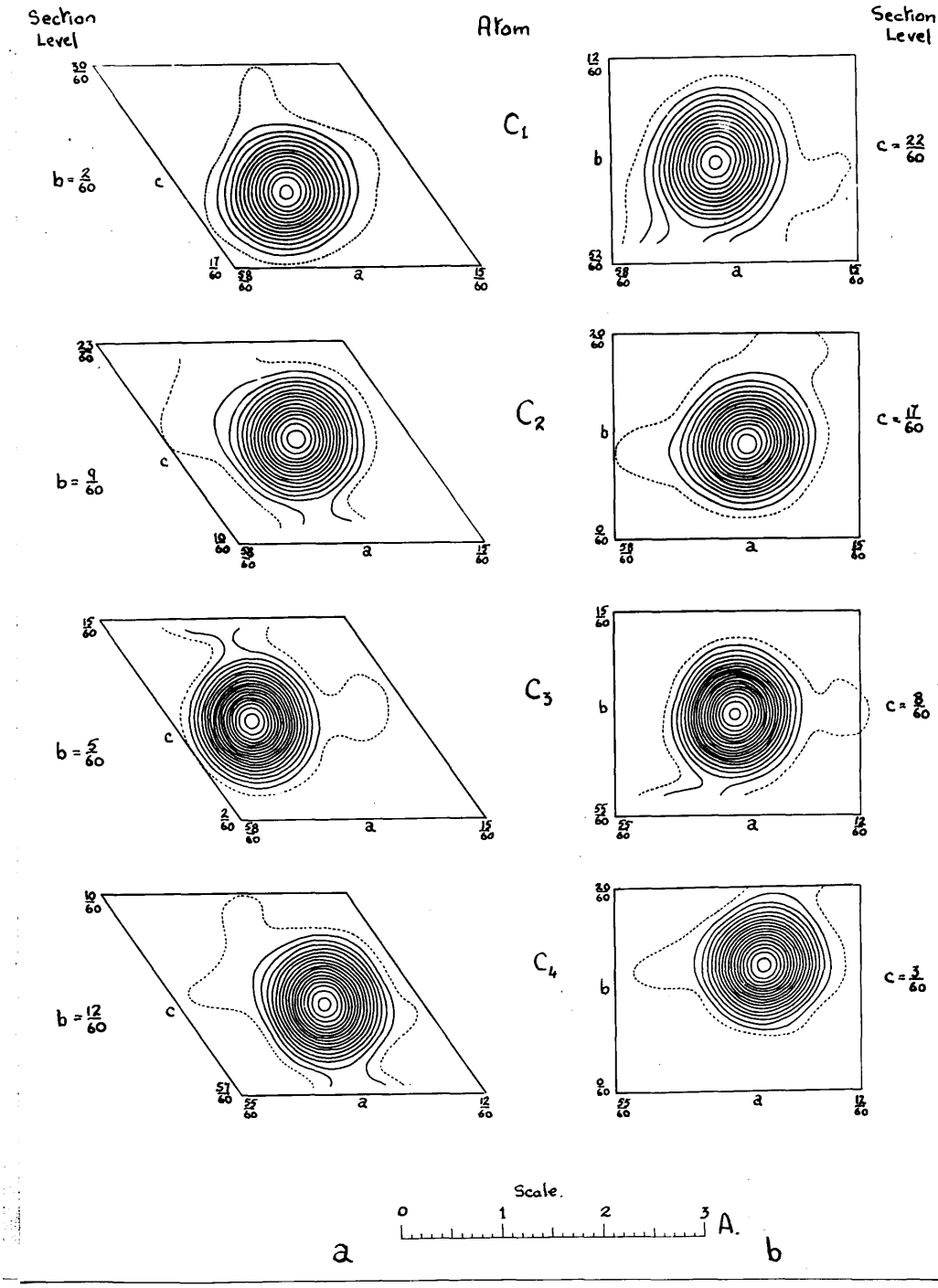

Fig. 3a and b. Sections through C_1 of the anthracene molecule.
Fig. 4a and b. Sections through C_2 of the anthracene molecule.
Fig. 5a and b. Sections through C_3 of the anthracene molecule.
Fig. 6a and b. Sections through C_4 of the anthracene molecule.
In all figures a is parallel with (010), and b is parallel with (001). Each contour line represents a density increment of one half electron per A^3, the half electron line being dotted.

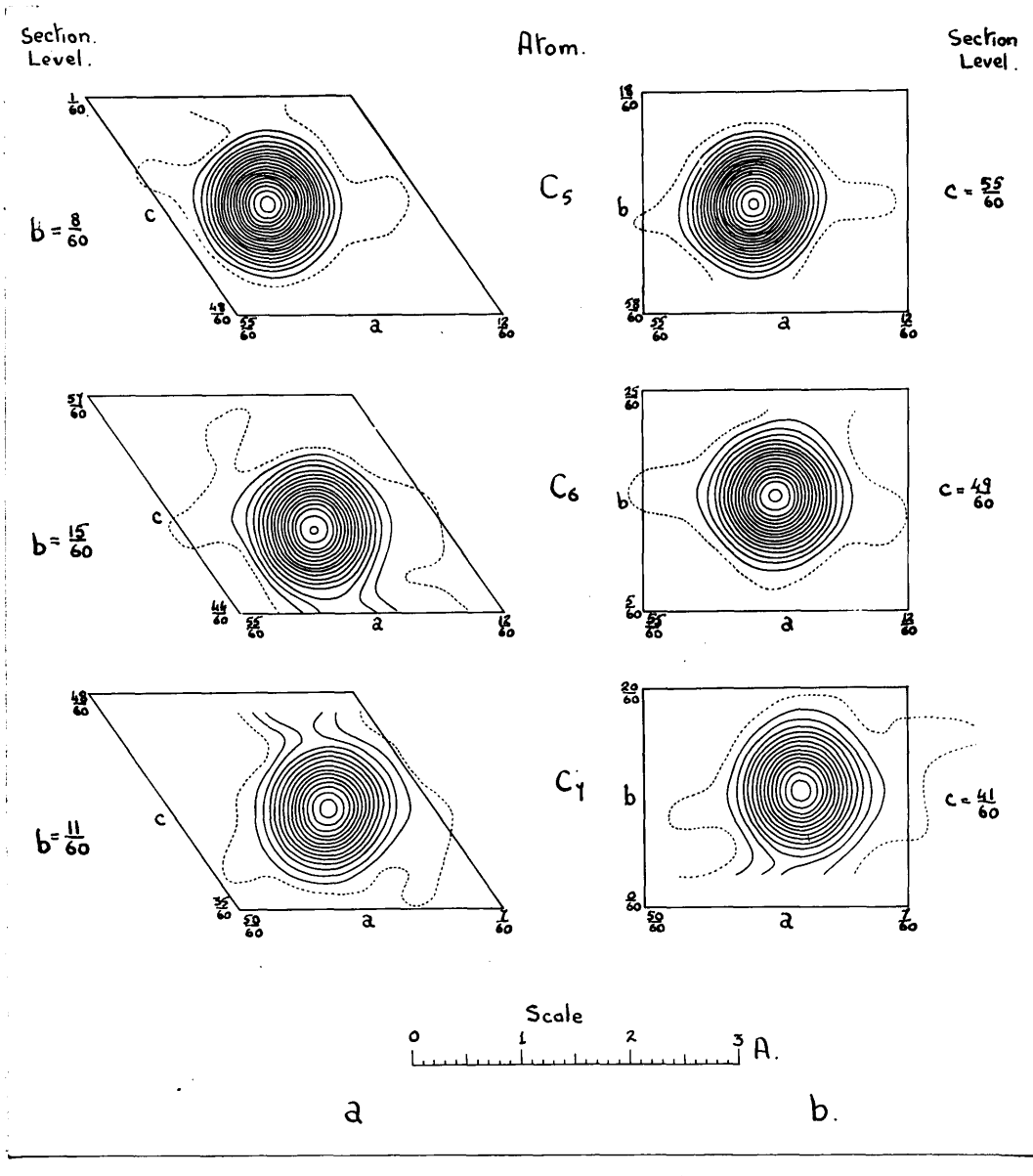

Fig. 7a and b. Sections through C_5 of the anthracene molecule.
Fig. 8a and b. Sections through C_6 of the anthracene molecule.
Fig. 9a and b. Sections through C_7 of the anthracene molecule.
In all figures a is parallel with (010), and b is parallel with (001). Each contour line represents a density increment of one half electron per A^3, the half electron line being dotted.

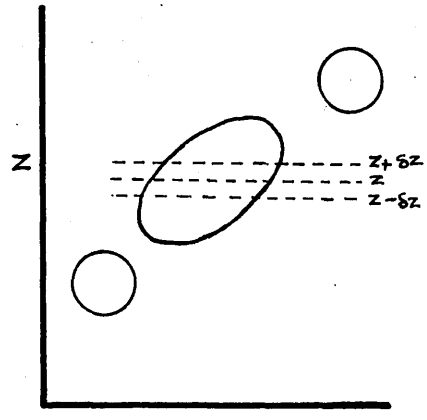

To illustrate this in a very general way, we can consider the exaggerated case of atom A in the vicinity of atoms B and C. If sections are drawn through atom A parallel to the (001) plane at z, z+δz, and z-δz, where z is the true z co-ordinate of the atom, then it is apparent that the x and y co-ordinates of the centres given by the sections at z+δz, and z-δz will differ appreciably from the true atomic centre. Thus it is very important that in finding atomic co-ordinates from sections drawn at various levels throughout the unit cell, that more than one section should be drawn for each atom, and that these should be selected on either side of the atomic centre. This effect does not arise in two dimensional determinations, since there one is considering the projection of the atom.

The x, y, and z co-ordinates which were accurately determined from these sections are collected in Table V together with the individual errors in estimating the atomic centres. (The x co-ordinate given is the mean of eight values estimated from the sections through each atom).

Table V

Atomic co-ordinates in Angstrom units, the centre of symmetry being taken as origin.

	xA	yA	zA
C_1	0.7360 ± .0064	0.1714 ± .0018	4.0636 ± .0029
C_2	1.0100 ± .0030	0.9387 ± .0043	3.1205 ± .0032
C_3	0.5073 ± .0038	0.4988 ± .0007	1.5441 ± .0032
C_4	0.7407 ± .0005	1.2464 ± .0029	0.5295 ± .0020
C_5	0.2569 ± .0032	0.7914 ± .0006	-1.0006 ± .0018
C_6	0.5133 ± .0005	1.5461 ± .0048	-2.0324 ± .0018
C_7	0.0207 ± .0014	1.0668 ± .0050	-3.5301 ± .0029

In Table VI these co-ordinates are expressed as fractions of the axial lengths in degrees, and also given in terms of a, b, and c', where c' is an axis drawn perpendicular to a and b. The co-ordinates referred to orthogonal axes are useful in deriving the inter-atomic distances and bond angles, and they are obtained from the co-ordinates referred to the monoclinic crystal axes by the relations

$x' = x - z\sin 34^\circ 42'$

$z' = z\cos 34^\circ 42'$

Table VI.

	x'A	$2\pi\frac{x}{a}$	$2\pi\frac{y}{b}$	z'A	$2\pi\frac{z}{c}$
C_1	-1.5774	30.99°	10.23°	3.3407	131.20°
C_2	-0.7665	42.52	56.05	2.5654	100.75
C_3	-0.3718	21.36	29.78	1.2694	49.85
C_4	0.4393	31.18	74.42	0.4353	17.10
C_5	0.8265	10.82	47.26	-0.8266	-32.31
C_6	1.6703	21.61	92.32	-1.6708	-65.62
C_7	2.0304	0.87	63.70	-2.9021	-113.98

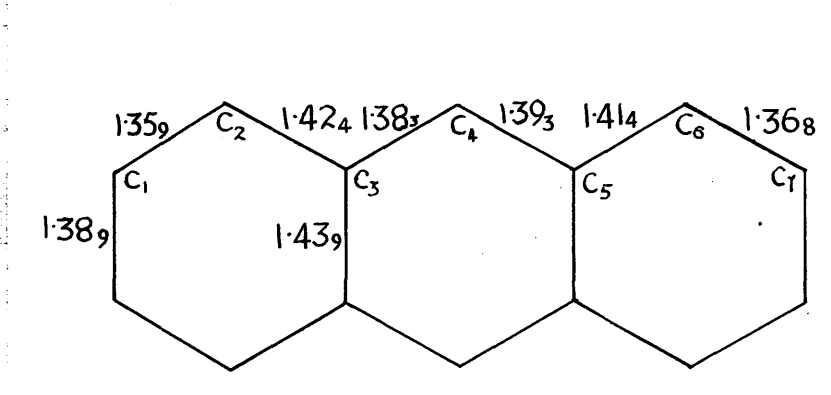

Fig. 10. Measured bond lengths in the anthracene molecule.

Table VII.

Inter-atomic distances and valency angles from the atomic co-ordinates.

C$_1$ - C$_2$	1.35 A	C$_2$ $\hat{C}$ C$_1$ C$_7$'	121° 18'
C$_2$ - C$_3$	1.42	C$_1$ $\hat{C}$ C$_2$ C$_3$	120° 42'
C$_3$ - C$_4$	1.38	C$_2$ $\hat{C}$ C$_3$ C$_5$'	118° 12'
C$_4$ - C$_5$	1.39	C$_4$ $\hat{C}$ C$_3$ C$_5$'	118° 54'
C$_5$ - C$_6$	1.41	C$_3$ $\hat{C}$ C$_4$ C$_5$	122° 02'
C$_6$ - C$_7$	1.36	C$_4$ $\hat{C}$ C$_5$ C$_3$'	119° 02'
C$_7$ - C$_1$'	1.38	C$_6$ $\hat{C}$ C$_5$ C$_3$'	118° 46'
C$_3$ - C$_5$'	1.43	C$_5$ $\hat{C}$ C$_6$ C$_7$	120° 47'
		C$_6$ $\hat{C}$ C$_7$ C$_1$'	120° 50'

It will be observed in Fig. 10 that pairs of bonds, which, although crystallographically distinct are not chemically distinct, show a variation from their mean value of .005A, and it is therefore estimated that the maximum error in bond lengths is .010A. Thus the variations in the averaged values shown in Fig. 11 will be significant.

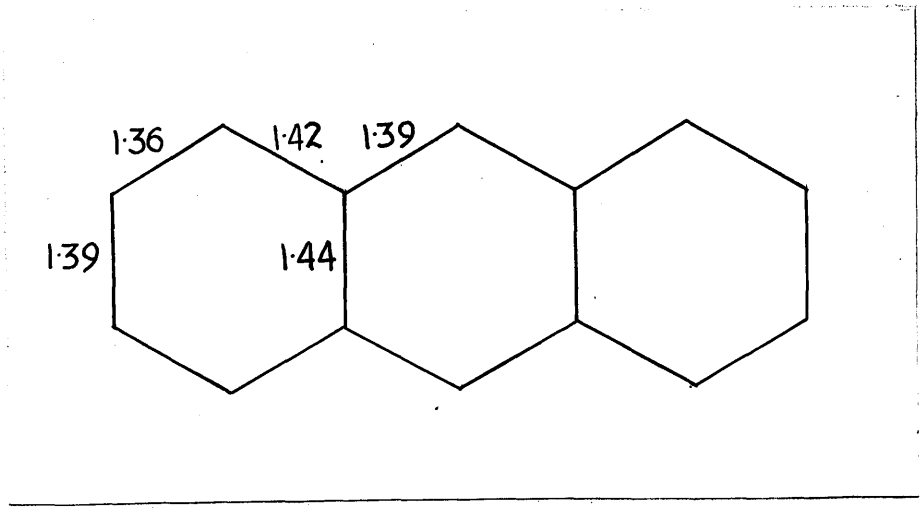

Fig. 11. Averaged bond lengths in the anthracene molecule.

The central $C_3 - C'_5$ bond is very much longer than the normal accepted value of 1.40A for the carbon-carbon distance in the aromatic ring, and this variation is in harmony with resonance considerations.

The shortening of the $C_1 - C_2$ bond is similar to the contraction found for this position in naphthalene. Modern theories of chemical reactivity in the aromatic ring indicate that the ease of addition reactions gives a measure of the double bond character in a linkage and one would therefore expect that addition to the 1:2 positions in naphthalene and anthracene would produce the most stable derivatives.

This predicts correctly the derivatives of naphthalene where the 1:2 compound is always formed, but in anthracene it is the "meso" compound which is usually obtained. A possible explanation of this anomaly has been suggested by Gold (1948). It is that the 1:2 compound is not isolated because the 9:10 addition proceeds more rapidly by a different mechanism, and thermodynamic equilibrium between the two forms is not attained.

Another explanation is that some form of ring strain prevents the formation of the 1:2 derivative.

The valency angles are all very close to the angles of regular hexagon rings except $C_3 \widehat{C_4} C_5$ which has increased to 122°. This appears to indicate that the central ring opens out to accommodate the long $C_3 C_5'$ bond. Measurement of the distance between atoms C_4 and C_4' confirms this theory. This inter-atomic distance is 2.78A, which is much less than twice the length of bond $C_3 C_5'$.

Electron Density in the Molecular Plane.

From the co-ordinates listed in Table VI it was calculated that the atoms all lay near a mean plane given by the equation

$$x - .5329y - .1584z = 0$$

with respect to the monoclinic crystal axes.

The distances of each atom from this plane are

Fig. 12. Contour map of electron density distribution in the plane of the anthracene molecule. Each contour line represents a density increment of one half electron per A^3, the half electron line being dotted.

given in Table VIII. These deviations are very small, and apparently random, and it is difficult to say whether or not they have any physical significance.

Table VIII.

Distances of atomic centres from the mean plane of the anthracene molecule.

C_1 +.0008A	C_4 -.0059A
C_2 +.0125A	C_5 -.0051A
C_3 -.0026A	C_6 +.0091A

C_7 +.0092A

The positive or negative sign indicates whether the atomic centres lie above or below the mean plane.

The electron density distribution was calculated for this plane and is shown in Fig. 12. The bond lengths and valency angles were measured directly from this section and the values obtained are given in Table IX.

These measured inter-atomic distances are probably less reliable than the calculated values, as only one estimation of the atomic centre was made for each atom, compared with at least four estimations in the determination of the atomic co-ordinates. Since the deviations of the atoms

Table IX.

Inter-atomic distances and valency angles from the section through the plane of the molecule.

$C_1 - C_2$	1.36 A	$C_2 \hat{C}_1 C'_7$	121° 00'
$C_2 - C_3$	1.42	$C_1 \hat{C}_2 C_3$	120° 45'
$C_3 - C_4$	1.38	$C_2 \hat{C}_3 C'_5$	117° 55'
$C_4 - C_5$	1.39	$C_4 \hat{C}_3 C'_5$	119° 00'
$C_5 - C_6$	1.41	$C_6 \hat{C}_5 C_3$	119° 00'
$C_6 - C_7$	1.36	$C_5 \hat{C}_6 C_7$	120° 40'
$C_7 - C'_1$	1.39	$C_6 \hat{C}_7 C'_1$	120° 45'
$C_3 - C'_5$	1.44		

from the plane are so small the error introduced by assuming the planarity of the molecule is probably negligible.

An interesting feature of this electron density map is that the hydrogen atoms are clearly indicated on carbon atoms C_1, C_2, C_4, C_6 and C_7 and the hydrogen on C_6 is completely resolved, giving a carbon-hydrogen bond of 1.10A. The general arrangement of the molecules in the unit

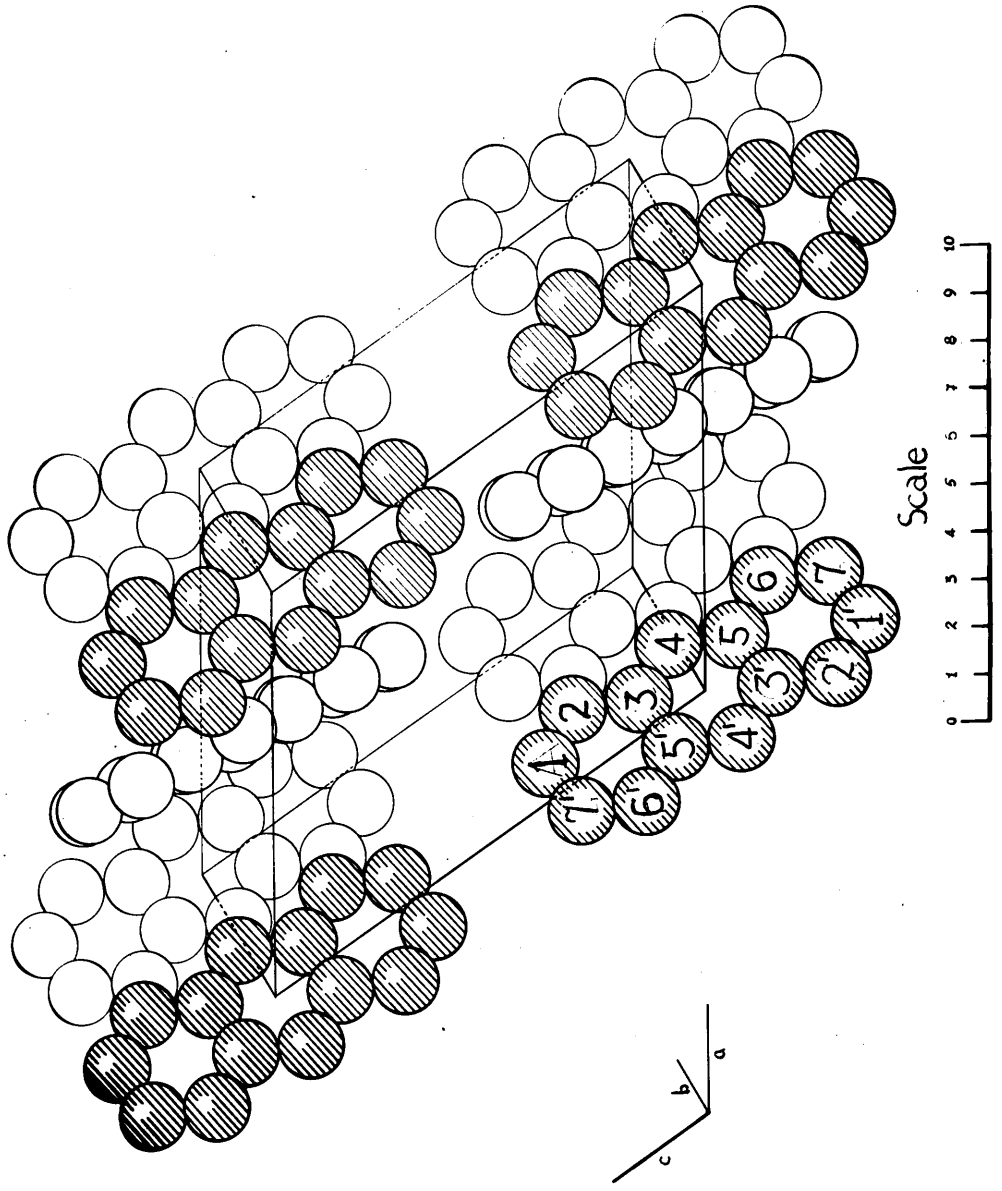

Fig. 13. The arrangement of the anthracene molecules in the crystal lattice.

cell of anthracene is shown in Fig. 13.

Electron Distribution.

It had previously been noticed in anthracene (Robertson 1933) that the peak electron density varied throughout the molecule, being highest for the atoms in the "meso" position, and least for the atoms in the "benz" position. In the present structural determination the falling off in peak electron density as one moves outwards from the centre of the molecule is very pronounced. Values are shown in Table X.

Table X.

Peak values for the electron density in anthracene.

C_1	7.5 electrons per A^3	C_4	9.0
C_2	8.0	C_5	9.0
C_3	9.5	C_6	8.5
	C_7 7.5		

Together with this effect there is the noticeable feature that for the atoms of the outer ring, the electron contours are very much less circular than for the atoms of the central ring, and the bridges between atoms $C_1 C'_7$, $C_1 C_2$, and

$C_6 C_7$ have a density of 2 electrons per A^3 compared with bridge values of 1 electron for the bonds between atoms $C_3 C_4$ and atoms $C_3 C_5$.

These features in the outer ring may be due to thermal agitation. If the molecule is oscillating about its centre, the effect would be most marked in the outlying atoms and consequently give rise to this slight blurring effect. Additional evidence in favour of this view is that the binding forces between the ends of molecules appear to be relatively weaker than those between the sides of neighbouring molecules. This is illustrated by the fact that the (001) plane is the most important natural face of the crystal, and is also the cleavage plane.

Spectroscopic studies of anthracene appear to offer some support to this hypothesis. It has been observed that the absorption bands at normal temperatures are very flattened compared with those obtained at low temperatures, which suggests that the diffuseness is due to thermal vibration. It is, however, impossible to draw a strict analogy between substances in the crystalline state and in solution.

These effects may also be closely linked with the chemistry of the molecule. In most reactions with anthracene the central benzene ring is the first to be attacked by substituents, and there is probably some relation between

this fact and the observed enhanced electron density in the central ring.

Discussion.

The most striking result of this analysis is the comparatively large variation in bond lengths found within the anthracene molecule, and it is of interest to draw a comparison between the experimental results and the inter-atomic distances derived from quantum mechanical treatments.

A purely qualitative approach is by a consideration of the four Kekulé structures (Pauling, Brockway and Beach 1935).

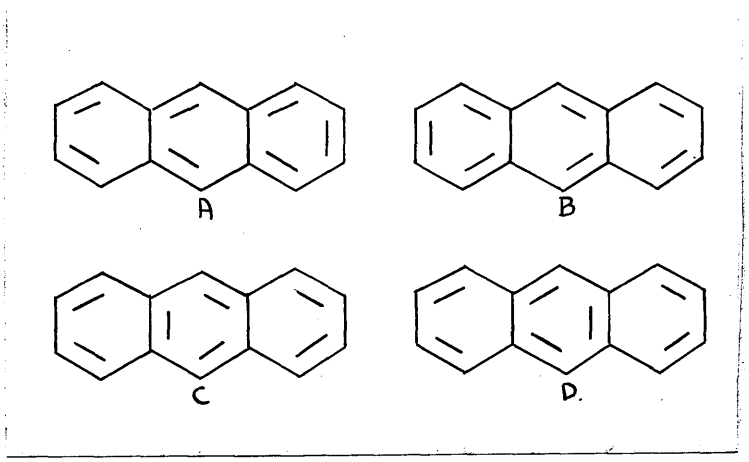

Fig. 14. The four Kekulé structures for anthracene.

The amount of double bond character for each link is easily obtained by inspection and by application of an empirical curve (Pauling 1937), which relates the inter-atomic

distance to the amount of double bond character in a single bond - double bond resonance system, the bond lengths may be obtained. The results of such a calculation are illustrated in Fig. 15.

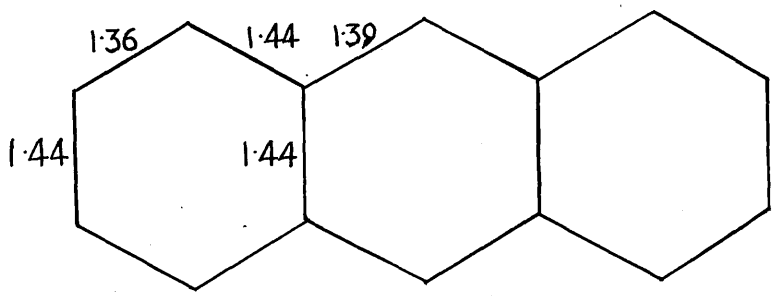

Fig. 15. Calculated bond lengths based on the Kekulé structures for the anthracene molecule.

Forster (1938) in his valence bond treatment of anthracene regards the ground state and the lowest excited state as combinations of the four unexcited structures.

The wave functions Ψ_I and Ψ_{II} are of the form

$$\Psi_I = c_1(\Psi_A + \Psi_B) + c_2(\Psi_C + \Psi_D)$$

$$\Psi_{II} = c_3(\Psi_A - \Psi_B) + c_4(\Psi_C - \Psi_D)$$

having c_1 - - - - c_4 as determined numerical constants.

It has been shown, however, that excited structures are very significant even in the ground state. There are forty eight mono-excited structures for anthracene of the form

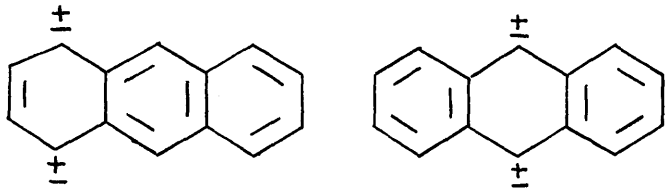

Svartholm and Jonnson (1941) have shown that these are six times more important than the unexcited structures.

A more comprehensive determination of bond lengths by the molecular orbital method (Coulson 1939, 1941, Coulson and Lennard Jones 1939) includes all these mono-excited structures. This method is based on the principle that, in a molecule, the outer unpaired electrons are not localised about one nucleus, but are associated with all the others (Huckel 1931). Thus all the electrons in a molecule are regarded as belonging to the whole nuclear framework, and not to particular nuclei. In practice, however, it is sufficiently accurate to consider the molecular orbitals of electrons as localised between two or more centres.

The empirical relationship between bond order and bond length has been widely used to predict the length of a

bond of known order. A smooth curve is drawn through points corresponding to single, double and triple bonds, and through the points representing benzene and graphite. It is then possible to read off from this, any required bond length once the order of the link has been calculated. The same values are used to define this bond order-bond length curve as for Pauling's curve (1937) relating bond length and double bond character.

In the molecular orbital treatment, the order of a bond in an aromatic compound is considered as being composed of two parts. One part of magnitude unity, is provided by the fixed localised bonds, and the other part, p, is contributed by the mobile π electrons. The total order is, therefore, 1 + p. The contribution p depends on the density of the mobile electrons in the region between the two atoms forming the bond. This is correlated with the individual wave functions. Thus, in general, a given electron with wave function

$$\Psi = a_1\Psi_1 + a_2\Psi_2 + \cdots\cdots\cdots + a_n\Psi_n$$

will make a contribution to all the bonds. If a_r and a_s are both large, there will be a large probability of finding the electron on nuclei r and s. Therefore the contribution of an electron to the order of the bond r - s may be defined

as $a_r a_s$. Then the total order p is the sum of the contributions $a_r a_s$ from each mobile electron and may be calculated if the co-efficients $a_1, a_2, \ldots a_n$ of the wave function are known. These are obtained by solution of a rather complicated determinantal equation.

Coulson does not give results for the bond lengths of anthracene, but from values of bond orders (Coulson and Daudel 1947), the bond lengths shown in Fig. 16 were obtained.

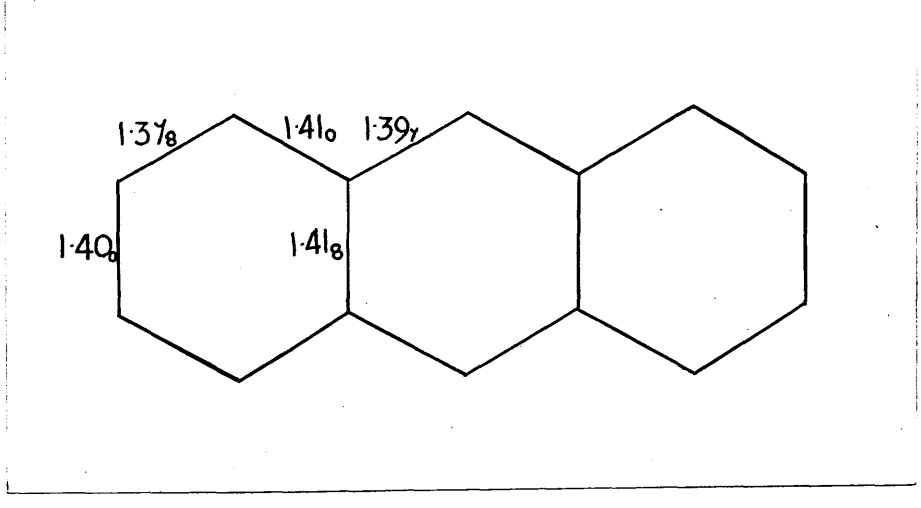

Fig. 16. Calculated bond lengths in anthracene (Coulson 1947).

Another, perhaps less rigorous, method of calculating bond lengths, is the electron pair method used by Penney (1937). The results obtained by this method agree very closely with those from molecular orbital calculations for naphthalene, but no calculations have, as yet, been made

for anthracene. This fact is not surprising when one considers that there are four hundred and twenty nine canonical structures for anthracene compared with a total of forty two for naphthalene. The rigorous solution of such a secular equation as was carried out by Sherman (1934) for naphthalene, would involve a considerable amount of labour.

An extension of the simple mesomerism theory has been made by Daudel (1948) to give a method of molecular diagrams. This treatment is essentially the same as Pauling's (1942) method of calculating percentage double bond character, except that higher excited as well as unexcited formulae are introduced.

The treatment is fairly simple, and from a theoretical point of view is quite rigorous. If we consider the formula of an aromatic molecule which possesses a double bond between the atoms 1 and m, then the importance of the sharing between the atoms 1 and m is given by

$$I_{lm} = \sum_i S_i$$

where S_i is the importance of the formula considered (proportional to the square of the co-efficient of the wave function). The number I_{lm} is called the "indice de liaison" of the bond 1-m.

If S_j is the importance of a formula possessing

an ineffective bond (i.e. a bond between two non-adjacent carbon atoms) leading to a certain atom l, then

$$J_l = \sum_j S_j$$

represents the amount of unshared electrons existing in the atom l, and is called the "indice de valence libre" (Daudel and Pullman 1945). Thus, by calculating the importances of all the possible formulae for a molecule, it is possible to set up a molecular diagram which indicates these indices.

Daudel uses an extension and simplification of the method of Pauling and Wheland (1933) to calculate these importances, and includes higher excited structures. The importance of these structures increases with increasing complexity of the molecule. In anthracene it is found that the importances of the unexcited, momo-excited and di-excited formulae are in the ratio of 10:60:30. The molecular diagram obtained for anthracene is shown in Fig. 17.

The amount of double bond character is obtained from this diagram from the formula

$$Y_{lm} = I_{lm} + a\left(J_l + J_m\right)_{\frac{l\ \ m}{2}}$$

where a is a constant = 1/2.

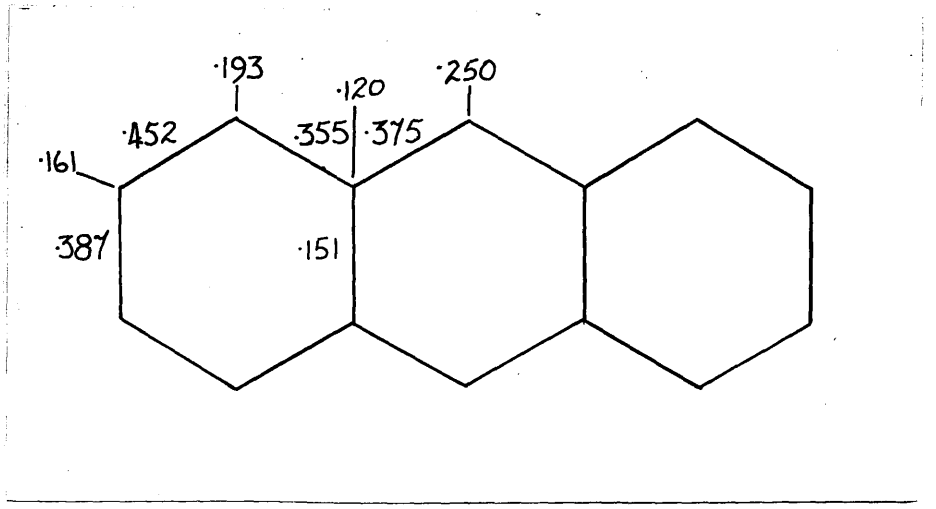

Fig. 17. Molecular Diagram for anthracene (Daudel 1948).

The inter-atomic distances can then be read off from Pauling's curve (1937). The results obtained for anthracene are shown in Fig. 18.

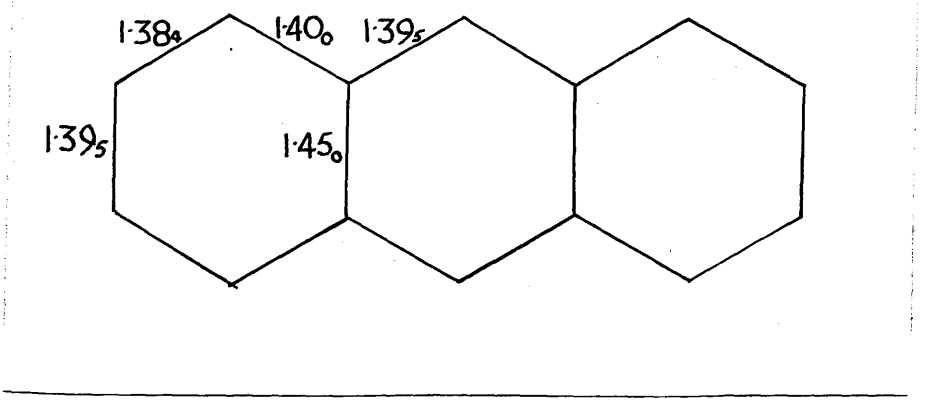

Fig. 18. Calculated bond lengths in anthracene (Daudel 1948).

It will be observed that the results of Coulson and Daudel are very similar, but, although they both place the inter-atomic distances in the correct sequence, the actual values of the bond lengths are not in perfect agreement with those determined experimentally. Indeed they appear no more reliable than those calculated by consideration of the simple Kekulé structures. This lack of precision in the quantum mechanical treatment may be due to inaccuracies in the curve relating double bond character and bond length (Daudel 1949), or to the fact that the treatment is not completely rigorous, some assumptions being necessary in order to simplify the calculations.

Table XI. Measured and Calculated Values of the Structure Factor.

hkl	sin θ	$F_{obs.}$	$F_{calc.}$	hkl	Sin θ	$F_{obs.}$	$F_{calc.}$
200	.219	65.0	+73.8	035	.567	16.6	+15.5
400	.438	3.9	- 1.8	036	.633	5.4	+ 2.9
600	.657	7.3	- 8.3	037	.703	2.2	- 2.2
800	.876	2.5	- 1.5	038	.776	3.5	- 2.7
020	.256	22.7	-22.5	039	.847	2.0	- 2.0
040	.512	3.7	- 1.6	0,3,10	.923	<1.2	+ 0.8
060	.768	<1.8	+ 1.8	041	.520	4.5	- 3.5
001	.084	32.8	+38.4	042	.540	<1.6	+ 0.8
002	.168	23.7	-25.2	043	.571	1.4	- 0.7
003	.252	16.4	+15.0	044	.612	1.9	- 0.5
004	.336	24.6	-19.9	045	.661	13.2	+12.5
005	.420	16.9	-14.7	046	.718	6.8	+ 5.8
006	.504	6.0	+ 6.0	047	.781	3.4	- 4.6
007	.588	<1.8	- 0.7	048	.847	1.5	- 1.4
008	.673	4.1	- 4.4	049	.912	2.3	- 1.9
009	.757	5.8	- 5.0	0,4,10	.983	2.6	- 2.1
0,0,10	.841	<1.8	- 0.7	051	.646	<1.8	- 1.1
0,0,11	.925	1.5	+ 1.7	052	.662	<1.8	+ 1.0
011	.152	10.7	+10.4	053	.688	11.3	- 9.4
012	.209	3.6	+ 3.4	054	.723	5.4	- 5.8
013	.280	3.9	- 3.2	055	.765	2.6	+ 3.2
014	.358	11.9	- 9.6	056	.815	<1.7	- 0.5
015	.435	16.0	-13.6	057	.870	2.6	+ 1.8
016	.518	<2.1	- 0.4	058	.929	3.8	+ 4.0
017	.600	3.6	+ 4.4	059	.989	<0.8	- 1.5
018	.683	9.0	- 8.5	061	.772	4.2	- 4.6
019	.767	9.8	- 9.2	062	.785	<1.8	- 1.6
0,1,10	.849	<2.0	- 0.3	063	.808	8.8	+ 8.9
0,1,11	.933	<1.3	- 0.3	064	.838	3.3	+ 2.5
021	.270	17.8	-18.9	065	.875	4.3	- 4.3
022	.305	8.7	+ 5.6	066	.919	4.0	- 1.8
023	.359	4.9	0.0	067	.968	<0.9	- 0.7
024	.421	17.9	-15.7	071	.899	3.5	- 2.4
025	.491	1.1	+ 1.8	072	.910	1.6	- 0.9
026	.565	<1.2	- 1.5	073	.930	<1.3	- 1.2
027	.640	<1.4	- 1.1	074	.956	<1.1	+ 0.8
028	.719	12.4	+10.9	075	.989	1.4	- 0.6
029	.797	4.1	+ 3.3	2,0,10	.977	<1.0	+ 0.9
0,2,10	.878	2.0	- 2.2	209	.896	4.3	- 5.7
0,2,11	.959	<0.9	+ 0.8	208	.815	5.5	- 7.5
031	.393	20.9	-18.7	207	.735	<2.2	- 0.3
032	.418	<1.3	- 0.4	206	.655	3.5	+ 4.0
033	.458	8.0	+ 6.9	205	.574	9.3	- 8.3
034	.509	14.4	+12.9	204	.496	25.5	-24.8

hkl	sin θ	$F_{obs.}$	$F_{calc.}$	hkl	sin θ	$F_{obs.}$	$F_{calc.}$
203	.417	4.4	- 2.5	$60\bar{7}$	.577	2.0	+ 2.3
202	.345	4.3	+ 3.1	$60\bar{8}$	.613	2.4	- 4.0
201	.274	4.5	- 4.1	$60\bar{9}$	.658	16.4	+19.0
$20\bar{1}$	.182	43.5	+52.8	$6,0,\bar{10}$	.708	16.6	+17.6
$20\bar{2}$	.184	25.5	-28.8	$6,0,\bar{11}$	.765	3.8	- 3.9
$20\bar{3}$	.219	14.5	+12.5	$6,0,\bar{12}$	.819	<2.0	0.0
$20\bar{4}$	.277	3.3	+ 2.4	$6,0,\bar{13}$	.895	<1.7	+ 1.9
$20\bar{5}$	.346	5.0	-10.5	$6,0,\bar{14}$	.965	3.0	- 3.2
$20\bar{6}$	.420	5.4	+ 7.4	802	.980	<1.0	- 1.1
$20\bar{7}$	.496	4.4	- 5.3	$80\bar{1}$	.922	<1.5	+ 0.5
$20\bar{8}$	.575	2.6	+ 3.0	$80\bar{1}$	.826	7.4	- 8.7
$20\bar{9}$	.656	9.2	+10.4	$80\bar{2}$	.789	4.5	- 3.1
$2,0,\bar{10}$	.736	<1.6	+ 0.1	$80\bar{3}$	.756	2.1	+ 2.6
$2,0,\bar{11}$	.817	<1.5	+ 0.8	$80\bar{4}$	.733	<2.1	- 1.1
$2,0,\bar{12}$	.901	<1.2	- 0.2	$80\bar{5}$	.720	10.3	- 9.6
$2,0,\bar{13}$	.981	<0.7	- 5.2	$80\bar{6}$	.714	9.0	- 8.1
408	.987	3.2	- 4.2	$80\bar{7}$	.720	2.2	+ 2.6
407	.910	<1.5	0.0	$80\bar{8}$	.735	<2.1	- 0.7
406	.835	<1.8	+ 0.8	$80\bar{9}$	.757	2.1	+ 1.9
405	.760	<2.1	- 1.8	$8,0,\bar{10}$	.790	9.0	+ 9.0
404	.687	8.4	- 7.9	$8,0,\bar{11}$	.830	<1.9	- 0.4
403	.617	7.6	- 8.0	$8,0,\bar{12}$	.869	1.4	- 1.4
402	.553	3.7	+ 5.1	$8,0,\bar{13}$	.927	1.5	+ 2.8
401	.490	<1.7	- 1.1	$8,0,\bar{14}$	.984	<1.0	- 1.3
$40\bar{1}$	.394	3.5	+ 7.5	$10,0,\bar{3}$	.968	<1.1	+ 0.9
$40\bar{2}$	.365	6.3	- 7.2	$10,0,\bar{4}$	.989	<1.4	- 1.2
$40\bar{3}$	.359	6.2	+ 5.1	$10,0,\bar{5}$	.917	<1.5	- 0.9
$40\bar{4}$	.368	1.8	+ 1.1	$10,0,\bar{6}$	.900	<1.7	- 3.3
$40\bar{5}$	.396	12.3	-13.9	$10,0,\bar{7}$	.894	<1.7	- 0.5
$40\bar{6}$	.439	5.0	+ 6.0	$10,0,\bar{8}$	.894	<1.7	+ 1.7
$40\bar{7}$	.491	5.2	- 5.0	$10,0,\bar{9}$	.902	1.9	- 2.7
$40\bar{8}$	.552	1.6	+ 0.6	$10,0,\bar{10}$	.919	1.8	- 2.3
$40\bar{9}$	.619	26.6	+28.3	$10,0,\bar{11}$	.942	<1.4	- 0.5
$4,0,\bar{10}$	.687	10.3	+10.3	$10,0,\bar{12}$	.972	<1.1	0.0
$4,0,\bar{11}$	.761	3.7	- 3.7	$1,\bar{1},1,1$	.993	<0.9	+ 0.3
$4,0,\bar{12}$	.837	2.0	+ 2.0	$1,\bar{1},1,0$	.928	<1.5	0.0
$4,0,\bar{13}$	.915	3.6	- 3.1	$11\bar{9}$	.884	2.4	- 2.4
$4,0,\bar{14}$	.994	<2.0	- 4.8	$11\bar{8}$	.751	<2.1	+ 0.4
605	.957	<1.2	- 1.2	$11\bar{7}$	.672	<1.7	- 0.1
604	.890	4.5	+ 3.5	$11\bar{6}$	.589	<1.7	+ 0.8
603	.825	<2.0	+ 0.1	$11\bar{5}$	.509	6.4	- 5.7
602	.764	<2.1	- 0.7	$11\bar{4}$	.430	19.3	-17.1
601	.705	<2.1	+ 2.7	$11\bar{3}$	.351	6.0	+ 7.1
$60\bar{1}$	.609	11.2	-12.8	$11\bar{2}$	.281	<1.0	- 1.1
$60\bar{2}$	.574	2.9	- 3.1	$11\bar{1}$	.216	12.4	- 7.9
$60\bar{3}$	.551	4.9	+ 5.1	$11\bar{0}$	.168	53.5	+65.0
$60\bar{4}$	.538	4.6	- 2.4	$11\bar{1}$	.158	26.9	+29.4
$60\bar{5}$	.539	20.6	-18.4	$11\bar{2}$	.189	13.2	-14.5
$60\bar{6}$	.552	5.3	- 4.0	$11\bar{3}$	.247	15.5	+12.6

hkl	Sin θ	$F_{obs.}$	$F_{calc.}$	hkl	Sin θ	$F_{obs.}$	$F_{calc.}$
$11\bar{4}$	.316	21.1	-17.0	$31\bar{6}$	.433	< 1.6	+ 2.7
$11\bar{5}$	.392	19.5	-16.7	$31\bar{7}$	.497	0.9	- 2.7
$11\bar{6}$	.469	< 1.4	+ 1.5	$31\bar{8}$	.564	3.8	+ 3.9
$11\bar{7}$	.550	< 1.6	- 1.0	$31\bar{9}$	.638	13.7	+13.0
$11\bar{8}$	.628	6.7	+ 5.3	$3,1\bar{1}0$	.716	< 1.4	- 0.4
$11\bar{9}$	.711	3.6	+ 2.3	$3,1\bar{1}1$	.790	1.9	- 1.2
$1,1\bar{1}0$	.766	2.8	- 2.8	$3,1\bar{1}2$	.869	1.8	+ 1.8
$1,1\bar{1}1$	.874	< 1.4	+ 1.1	$3,1\bar{1}3$	.953	3.5	- 2.7
$1,1\bar{1}2$	.958	< 1.0	- 0.8	417	.919	< 1.5	+ 2.3
2,110	.988	< 0.9	- 0.1	416	.844	1.9	- 2.6
219	.904	< 1.6	- 1.1	415	.770	3.3	+ 1.5
218	.825	< 2.0	- 0.7	414	.697	10.5	+10.7
217	.746	< 2.2	+ 1.7	413	.633	5.0	+ 3.1
216	.668	< 2.2	- 1.7	412	.570	< 2.0	- 1.0
215	.589	< 1.5	- 1.9	411	.506	2.4	+ 2.7
214	.512	1.9	+ 0.9	410	.456	28.3	-24.9
213	.436	4.0	- 4.0	$41\bar{1}$	.414	33.1	-36.1
212	.368	3.8	+ 5.3	$41\bar{2}$	.387	2.7	+ 3.3
211	.303	1.7	+ 0.4	$41\bar{3}$	.381	5.2	+ 7.3
210	.253	52.0	-47.8	$41\bar{4}$	.390	16.4	-16.8
$21\bar{1}$	.223	40.5	-42.3	$41\bar{5}$	.416	10.2	- 7.6
$21\bar{2}$	.224	9.1	+ 8.5	$41\bar{6}$	.457	2.0	+ 2.0
$21\bar{3}$	.254	1.2	+ 3.0	$41\bar{7}$	.508	1.8	- 2.8
$21\bar{4}$	.305	6.9	- 6.8	$41\bar{8}$	.570	3.1	+ 4.2
$21\bar{5}$	.369	13.2	+11.5	$41\bar{9}$	.633	9.4	+10.4
$21\bar{6}$	.439	2.4	+ 3.5	$4,1\bar{1}0$	.702	3.1	+ 2.6
$21\bar{7}$	.515	6.5	- 7.3	$4,1\bar{1}1$	.770	2.2	- 2.3
$21\bar{8}$	.589	11.9	+11.0	$4,1\bar{1}2$	.849	< 1.9	+ 0.8
$21\bar{9}$	.667	16.5	+17.5	$4,1\bar{1}3$	.924	< 1.5	- 1.6
$2,1\bar{1}0$	.746	2.9	+ 2.7	516	.938	< 1.4	- 0.9
$2,1\bar{1}1$	.830	2.0	- 1.8	515	.869	1.8	+ 1.5
$2,1\bar{1}2$	.909	< 1.2	+ 1.0	514	.800	2.9	+ 3.0
$2,1\bar{1}3$	.988	1.7	- 1.8	513	.731	3.1	- 3.2
319	.988	< 0.9	- 2.1	512	.672	< 1.7	+ 0.5
318	.909	< 1.6	- 2.5	511	.613	< 2.1	+ 0.2
317	.830	2.0	- 0.4	510	.564	5.0	- 5.6
316	.756	2.1	- 0.3	$51\bar{1}$	.516	6.0	+ 5.4
315	.677	2.2	+ 1.4	$51\bar{2}$	.487	4.1	+ 2.9
314	.603	6.4	- 5.8	$51\bar{3}$	.469	1.6	- 0.8
313	.530	4.8	- 3.9	$51\bar{4}$	.446	3.8	- 3.2
312	.465	4.0	+ 5.4	$51\bar{5}$	.478	16.2	-15.2
311	.404	8.1	-10.0	$51\bar{6}$	.502	< 1.3	- 0.3
310	.352	11.7	+10.8	$51\bar{7}$	.540	2.0	+ 2.2
$31\bar{1}$	.314	31.5	+28.9	$51\bar{8}$	.584	2.8	- 3.5
$31\bar{2}$	.297	3.9	- 3.8	$51\bar{9}$	.643	12.5	+13.3
$31\bar{3}$	.303	2.6	+ 2.7	$5,1\bar{1}0$	.702	7.4	+ 7.7
$31\bar{4}$	.331	14.3	- 9.3	$5,1\bar{1}1$	.766	3.0	- 3.0
$31\bar{5}$	.377	25.8	-20.7	$5,1\bar{1}2$	.825	2.9	+ 2.1

hkl	sin θ	$F_{obs.}$	$F_{calc.}$	hkl	sin θ	$F_{obs.}$	$F_{calc.}$
$5,1,\bar{13}$	.909	< 1.6	-1.0	$8,1,\bar{4}$	.746	< 2.2	-1.8
$5,1,\bar{14}$	.983	3.2	-3.5	$8,1,\bar{5}$	.731	5.5	+3.7
615	.968	< 1.1	+0.3	$8,1,\bar{6}$	.726	3.5	+2.0
614	.899	8.2	+8.5	$8,1,\bar{7}$	.731	< 2.1	-0.5
613	.834	7.4	+6.3	$8,1,\bar{8}$	.746	< 1.2	+1.8
612	.775	< 1.6	-1.6	$8,1,\bar{9}$	.770	7.1	-6.1
611	.716	< 2.2	+0.4	$8,1,\bar{10}$	.800	12.5	-11.6
610	.672	6.2	-3.7	$8,1,\bar{11}$	.839	2.3	-1.8
$61\bar{1}$	.623	12.6	-10.9	$8,1,\bar{12}$	.879	2.1	+2.3
$61\bar{2}$	.589	< 1.1	-0.1	$8,1,\bar{13}$	.933	1.7	-1.8
$61\bar{3}$	.564	2.0	+3.2	$8,1,\bar{14}$	.993	< 0.7	-0.9
$61\bar{4}$	.555	6.0	-7.2	910	.993	< 0.8	-0.4
$61\bar{5}$	.555	5.9	-6.3	$91\bar{1}$	.948	4.3	-3.6
$61\bar{6}$	.570	1.8	-1.5	$91\bar{2}$	.904	1.7	-1.4
$61\bar{7}$	.593	1.5	+1.0	$91\bar{3}$	.869	< 1.7	-0.2
$61\bar{8}$	.628	< 2.0	+1.4	$91\bar{4}$	.844	< 2.0	+0.4
$61\bar{9}$	.672	4.5	-4.2	$91\bar{5}$	.825	< 2.1	+1.0
$6,1,\bar{10}$	.721	6.1	-5.4	$91\bar{6}$	.820	2.4	-2.7
$6,1,\bar{11}$	.770	< 0.8	-0.9	$91\bar{7}$	.815	< 2.0	+0.2
$6,1,\bar{12}$	.830	< 2.0	+0.8	$91\bar{8}$	.825	< 1.9	+0.2
$6,1,\bar{13}$	.904	< 1.7	+0.5	$91\bar{9}$	.839	< 1.1	-2.4
$6,1,\bar{14}$	.973	1.5	+1.8	$9,1,\bar{10}$	.859	3.5	+3.6
713	.938	2.0	+1.6	$9,1,\bar{11}$	.889	2.0	+2.2
712	.879	2.1	-2.1	$9,1,\bar{12}$	.928	< 1.0	-0.9
711	.825	< 2.0	+1.9	$9,1,\bar{13}$	.978	< 0.7	+0.2
710	.775	3.0	-2.5	$10,1,\bar{3}$	.978	< 0.9	-0.6
$71\bar{1}$	.731	5.4	-4.2	$10,1,\bar{4}$	.948	< 1.4	-1.4
$71\bar{2}$	.692	< 1.7	+0.4	$10,1,\bar{5}$	.924	5.1	+5.8
$71\bar{3}$	.667	< 1.2	-0.3	$10,1,\bar{6}$	.909	8.4	+5.8
$71\bar{4}$	.647	< 1.5	+0.3	$10,1,\bar{7}$	.904	< 1.1	-0.6
$71\bar{5}$	.638	6.9	-5.8	$10,1,\bar{8}$	.904	< 1.6	+0.2
$71\bar{6}$	.643	3.7	-4.1	$10,1,\bar{9}$	.909	2.0	-1.5
$71\bar{7}$	.653	2.7	+3.6	$10,1,\bar{10}$	.928	7.6	-7.3
$71\bar{8}$	.682	3.1	-3.6	$10,1,\bar{11}$	.953	1.7	-2.4
$71\bar{9}$	.711	4.3	+2.9	$10,1,\bar{12}$	.978	< 1.0	+2.1
$7,1,\bar{10}$	.756	9.2	+9.4	$11,1,\bar{8}$	.993	< 0.5	+1.0
$7,1,\bar{11}$	.800	< 1.2	-0.2	$11,1,\bar{9}$	.993	< 0.8	-1.0
$7,1,\bar{12}$	.859	< 0.8	-0.2	1,2,10	.955	< 1.0	+1.2
$7,1,\bar{13}$	.914	< 1.6	+0.6	129	.911	3.2	-3.6
$7,1,\bar{14}$	.978	5.2	-3.4	128	.783	8.0	-7.4
812	.988	< 0.7	-0.1	127	.707	2.4	-1.6
811	.933	< 1.5	-0.6	126	.629	1.7	+0.8
810	.884	< 1.7	+0.6	125	.555	5.0	+5.0
$81\bar{1}$	.834	< 2.0	+0.8	124	.483	9.0	+6.9
$81\bar{2}$	.800	2.1	+2.1	123	.415	0.9	0.0
$81\bar{3}$	.766	< 2.0	-0.1	122	.357	< 0.5	+0.7

hkl	sin θ	$F_{obs.}$	$F_{calc.}$
121	.309	10.6	-10.8
120	.278	20.5	-22.1
12$\bar{1}$	.272	5.2	+1.3
12$\bar{2}$	.291	6.1	+8.6
12$\bar{3}$	.331	9.4	-9.8
12$\bar{4}$	.386	13.5	-9.4
12$\bar{5}$	.450	3.0	+5.0
12$\bar{6}$	.519	1.5	+2.9
12$\bar{7}$	.593	1.8	-2.6
12$\bar{8}$	.666	11.3	+8.9
12$\bar{9}$	.745	13.0	+10.9
12,$\bar{1}$0	.797	<1.2	-0.5
12,$\bar{1}$1	.902	<0.9	-0.3
12,$\bar{1}$2	.984	<0.6	+1.6
229	.931	<0.8	+0.2
228	.854	6.7	+7.4
227	.778	<1.3	+1.1
226	.703	2.1	-3.4
225	.629	11.2	+10.8
224	.558	5.4	+4.2
223	.489	2.8	-1.9
222	.429	6.2	+5.8
221	.375	13.3	-16.1
220	.337	13.1	-12.3
22$\bar{1}$	.314	4.4	+5.2
22$\bar{2}$	.315	0.7	+2.0
22$\bar{3}$	.337	<0.7	+1.1
22$\bar{4}$	.377	23.8	-23.0
22$\bar{5}$	.430	20.1	-20.6
22$\bar{6}$	.492	<0.6	-1.0
22$\bar{7}$	.559	<0.7	-0.3
22$\bar{8}$	.629	5.5	+5.8
22$\bar{9}$	.703	3.5	+2.5
2,2$\bar{1}$0	.778	4.7	-4.6
2,2$\bar{1}$1	.859	<1.2	+0.4
2,2$\bar{1}$2	.936	<0.8	+0.6
328	.936		-2.2
327	.859	1.2	-1.1
326	.788	<1.3	-1.0
325	.712	8.4	+6.5
324	.643	11.6	+11.6
323	.575	<1.2	-2.2
322	.515	1.2	-1.7
321	.461	2.1	+3.1
320	.416	28.1	-26.4
32$\bar{1}$	.385	24.7	-25.0
32$\bar{2}$	.370	4.7	+6.8
32$\bar{3}$	.375	3.8	+2.4
32$\bar{4}$	.399	10.6	-13.4
32$\bar{5}$	.437	6.3	+5.9
32$\bar{6}$	.486	9.7	+9.1
32$\bar{7}$	.544	3.2	-3.7
32$\bar{8}$	.611	1.3	+0.8
32$\bar{9}$	.675	8.8	+10.6
3,2$\bar{1}$0	.75	3.0	+3.9
3,2$\bar{1}$1	.821	<1.2	-1.0
3,2$\bar{1}$2	.897	<0.9	+1.5
3,2$\bar{1}$3	.979	<0.6	-1.3
427	.945	<0.8	+0.9
426	.873	<1.0	-2.3
425	.802	6.7	+6.6
424	.731	8.6	+8.3
423	.670	<1.3	-1.6
422	.611	1.1	+2.0
421	.553	4.7	-4.5
420	.507	2.2	-2.5
42$\bar{1}$	.470	20.8	+19.7
42$\bar{2}$	.446	5.8	+5.7
42$\bar{3}$	.441	4.2	-4.4
42$\bar{4}$	.448	4.5	-4.3
42$\bar{5}$	.472	19.3	-18.4
42$\bar{6}$	.508	5.9	-5.2
42$\bar{7}$	.554	2.4	+3.7
42$\bar{8}$	.611	2.3	-2.5
42$\bar{9}$	.670	2.7	-3.6
4,2$\bar{1}$0	.736	6.5	-5.4
4,2$\bar{1}$1	.802	<1.3	-0.6
4,2$\bar{1}$2	.878	<1.2	+1.4
4,2$\bar{1}$3	.950	2.2	-1.6
526	.964	<0.7	-1.0
525	.897	2.9	+1.8
524	.830	9.6	+9.4
523	.764	4.5	+3.0
522	.707	1.9	-3.3
521	.652	2.6	+4.1
520	.606	9.0	-7.1
52$\bar{1}$	.561	26.7	-21.2
52$\bar{2}$	.535	6.1	-4.4
52$\bar{3}$	.518	1.0	+2.4
52$\bar{4}$	.514	1.0	-3.0
52$\bar{5}$	.527	5.6	+3.3
52$\bar{6}$	.549	6.6	+5.7
52$\bar{7}$	.584	<1.2	0.0
52$\bar{8}$	.624	2.2	-3.8
52$\bar{9}$	.679	1.3	-0.5
5,2$\bar{1}$0	.736	1.8	+2.8

hkl	sin θ	$F_{obs.}$	$F_{calc.}$	hkl	sin θ	$F_{obs.}$	$F_{calc.}$
5,2,$\bar{11}$	.797	<1.3	+1.0	82$\bar{7}$	.764	<1.3	+0.4
5,2,$\bar{12}$	.854	<1.2	-0.5	82$\bar{8}$	.778	<1.3	-0.6
5,2,$\bar{13}$	.936	<0.9	-1.0	82$\bar{9}$	.802	2.7	-4.1
625	.993	<0.5	+1.8	8,2,$\bar{10}$	.830	2.5	+2.3
624	.926	3.6	+3.9	8,2,$\bar{11}$	.868	2.3	+2.1
623	.863	<1.0	-1.8	8,2,$\bar{12}$	.906	<0.9	-0.4
622	.806	<1.3	-0.7	8,2,$\bar{13}$	.909	2.2	-1.5
621	.750	<1.3	+0.9	92$\bar{1}$	.974	<0.7	-1.3
620	.707	<1.3	-1.0	92$\bar{2}$	.931	<0.9	-0.3
62$\bar{1}$	.661	13.4	+12.3	92$\bar{3}$	.897	<1.0	-0.7
62$\bar{2}$	.629	9.1	+7.9	92$\bar{4}$	.873	2.3	+0.9
62$\bar{3}$	.606	4.7	-6.3	92$\bar{5}$	.854	7.9	+7.5
62$\bar{4}$	.597	5.3	+5.6	92$\bar{6}$	.849	4.8	+3.8
62$\bar{5}$	.597	1.6	+2.0	92$\bar{7}$	.844	<1.2	-2.4
62$\bar{6}$	.611	3.4	-4.5	92$\bar{8}$	.854	<1.2	+1.7
62$\bar{7}$	.634	<1.3	+3.4	92$\bar{9}$	.868	2.5	-1.8
62$\bar{8}$	.666	2.8	-3.3	9,2,$\bar{10}$	.888	7.0	-7.8
62$\bar{9}$	.707	4.8	-6.4	9,2,$\bar{11}$	.916	2.1	-2.2
6,2,$\bar{10}$	.755	1.8	-2.1	9,2,$\bar{12}$	.955	<0.8	+1.1
6,2,$\bar{11}$	.806	<1.3	-0.2	9,2,$\bar{13}$	.998	<0.5	-1.8
6,2,$\bar{12}$	.859	<1.2	+1.2	10,2,$\bar{4}$	.974	<0.7	+0.7
6,2,$\bar{13}$	.931	4.1	-3.0	10,2,$\bar{5}$	.950	6.5	+5.7
723	.964	4.6	+4.0	10,2,$\bar{6}$	.936	<0.9	+1.0
722	.906	<0.9	-0.6	10,2,$\bar{7}$	.931	<0.9	-1.4
721	.854	<1.2	+0.9	10,2,$\bar{8}$	.931	<0.9	+0.9
720	.806	<1.3	-0.3	10,2,$\bar{9}$	.940	<0.9	-1.3
72$\bar{1}$	.764	8.3	-7.1	10,2,$\bar{10}$	.955	3.8	+3.3
72$\bar{2}$	.726	5.8	-4.5	10,2,11	.979	4.6	+4.2
72$\bar{3}$	.703	<1.3	0.0	1,3,10	.996	1.3	-2.1
72$\bar{4}$	.684	3.9	+2.7	139	.955	<1.0	-0.1
72$\bar{5}$	.675	8.2	+6.9	138	.833	8.0	+8.1
72$\bar{6}$	.679	2.5	+1.8	137	.763	<1.8	-0.9
72$\bar{7}$	.689	<1.3	-0.9	136	.691	2.9	+0.8
72$\bar{8}$	.717	<1.3	+0.3	135	.624	16.0	+16.7
72$\bar{9}$	.745	5.4	-5.9	134	.561	3.5	-2.3
7,2,$\bar{10}$	.788	4.8	-5.1	133	.504	13.4	-12.2
7,2,$\bar{11}$	.830	1.2	+1.2	132	.458	3.7	+4.6
7,2,$\bar{12}$	.888	<1.2	-0.1	131	.421	8.4	-7.1
7,2,$\bar{13}$	.940	3.0	-3.6	130	.399	21.5	-21.4
821	.909	<0.8	+1.5	13$\bar{1}$	.395	12.9	-14.9
820	.911	<0.9	-1.0	13$\bar{2}$	.408	<1.3	-0.1
82$\bar{1}$	.863	2.3	+1.9	13$\bar{3}$	.438	3.4	-3.6
82$\bar{2}$	.830	3.8	+4.6	13$\bar{4}$	.480	10.1	-10.3
82$\bar{3}$	.797	<1.3	-3.4	13$\bar{5}$	.533	8.9	+8.8
82$\bar{4}$	.778	3.7	+3.4	13$\bar{6}$	.592	8.1	+7.0
82$\bar{5}$	.764	8.4	+9.3	13$\bar{7}$	.658	4.3	-4.6
82$\bar{6}$	.759	<1.4	-0.4	13$\bar{8}$	.724	2.6	+2.5

hkl	sin θ	$F_{obs.}$	$F_{calc.}$
13$\bar{9}$	.798	< 1.7	+1.2
13$\bar{10}$	.847	1.6	-2.1
13$\bar{11}$	.946	< 1.1	+1.3
239	.974	2.8	-1.8
238	.901	5.6	-5.9
237	.829	4.6	-3.6
236	.759	2.4	+1.6
235	.691	11.4	+10.5
234	.627	13.6	+12.3
233	.566	5.5	+2.7
232	.516	1.0	+1.0
231	.472	6.8	-4.9
230	.442	3.7	-2.5
23$\bar{1}$	.425	12.4	+15.5
23$\bar{2}$	.426	2.2	+4.4
23$\bar{3}$	.442	3.5	-6.2
23$\bar{4}$	.473	1.1	-2.1
23$\bar{5}$	.517	4.6	-5.4
23$\bar{6}$	.569	2.1	-0.4
23$\bar{7}$	.627	< 1.5	+0.5
23$\bar{8}$	.691	3.2	-4.1
23$\bar{9}$	.759	< 1.6	-0.3
23$\bar{10}$	.829	< 1.4	+0.8
23$\bar{11}$	.905	< 1.2	-0.2
23$\bar{12}$	.978	< 0.8	+0.4
338	.978	4.0	+5.0
337	.905	4.1	+3.8
336	.838	< 1.2	-2.3
335	.768	8.0	+7.9
334	.703	5.5	+5.3
333	.642	6.2	-6.8
332	.589	1.3	+2.7
331	.542	0.9	-0.3
330	.505	7.5	-6.5
33$\bar{1}$	.479	4.3	-2.4
33$\bar{2}$	.468	5.6	-6.5
33$\bar{3}$	.472	2.5	+3.1
33$\bar{4}$	.491	3.3	+3.7
33$\bar{5}$	.522	3.2	-4.9
33$\bar{6}$	.564	2.1	+1.1
33$\bar{7}$	.615	< 1.3	-0.9
33$\bar{8}$	.674	4.5	-4.2
33$\bar{9}$	.733	3.7	-3.9
33$\bar{10}$	.802	2.3	-2.5
33$\bar{11}$	.869	1.1	+1.1
33$\bar{12}$	.941	1.8	-1.8
437	.987	2.4	-2.8
436	.919	< 1.3	+0.4
435	.851	3.1	+3.0
434	.785	6.5	+4.9
433	.729	2.6	+0.5
432	.674	< 1.8	-1.0
431	.622	1.1	+2.1
430	.582	1.8	-1.7
43$\bar{1}$	.550	< 1.4	-0.1
43$\bar{2}$	.529	< 1.3	+0.4
43$\bar{3}$	.525	< 1.3	-1.3
43$\bar{4}$	.532	9.3	+9.7
43$\bar{5}$	.552	10.4	+9.7
43$\bar{6}$	.583	3.5	+3.8
43$\bar{7}$	.623	< 1.7	+1.4
43$\bar{8}$	.674	4.9	-6.6
43$\bar{9}$	.729	2.7	-3.0
43$\bar{10}$	.789	3.6	+4.0
43$\bar{11}$	.851	< 1.7	+0.9
43$\bar{12}$	.923	< 1.3	-1.1
43$\bar{13}$	.992	< 0.6	-2.6
535	.941	< 1.2	+0.7
534	.878	2.2	+2.4
533	.816	< 1.7	-2.0
532	.763	< 1.6	+1.8
531	.712	< 1.8	-0.2
530	.670	1.2	-3.1
53$\bar{1}$	.630	8.7	+8.7
53$\bar{2}$	.606	< 1.6	+0.6
53$\bar{3}$	.592	< 1.5	-2.3
53$\bar{4}$	.589	13.1	+14.6
53$\bar{5}$	.599	< 1.5	+0.9
53$\bar{6}$	.619	8.1	-8.9
53$\bar{7}$	.650	< 1.2	+1.3
53$\bar{8}$	.687	2.0	-1.9
53$\bar{9}$	.737	6.9	-7.3
53$\bar{10}$	.789	4.8	-4.9
53$\bar{11}$	.847	< 1.6	0.0
53$\bar{12}$	.901	< 1.4	-0.8
53$\bar{13}$	.978	< 0.9	-3.2
634	.969	< 1.0	-0.3
633	.909	< 1.4	+0.5
632	.856	< 1.4	-0.8
631	.802	< 1.8	+2.0
630	.763	< 1.8	-1.2
63$\bar{1}$	.720	8.2	-6.8
632	.691	6.8	-5.2

hkl	sin θ	$F_{obs.}$	$F_{calc.}$	hkl	sin θ	$F_{obs.}$	$F_{calc.}$
$63\bar{3}$	.670	< 1.7	-0.1	$93\bar{9}$	.914	< 0.9	-1.2
$63\bar{4}$	.662	10.8	+9.1	$93\bar{10}$	.932	< 1.0	+0.2
$63\bar{5}$	.662	14.3	+12.2	$93\bar{11}$	.960	< 1.1	+0.1
$63\bar{6}$	.674	6.3	+4.3	$103\bar{5}$	.992	< 0.6	+1.0
$63\bar{7}$	.695	< 1.3	+1.2	$103\bar{6}$	.978	< 0.9	+0.1
638	.725	2.2	-2.5	$103\bar{7}$	.974	< 1.0	-0.6
$63\bar{9}$	.763	2.7	-3.0	$103\bar{8}$	.974	< 1.0	+0.7
$63\bar{10}$	.807	4.0	+4.1	$103\bar{9}$	.983	< 0.9	+0.5
$63\bar{11}$	.856	2.8	+2.8	$103\bar{10}$	.996	< 0.6	-1.8
$63\bar{12}$	.905	2.0	-1.9	148	.899	< 1.3	+0.8
$63\bar{13}$	.974	< 1.0	-1.5	147	.835	5.0	+1.0
732	.951	< 1.1	+1.1	146	.769	< 1.8	+1.4
731	.901	< 1.4	+0.4	145	.710	8.7	+7.7
730	.856	2.8	-4.2	144	.655	5.9	+4.3
$73\bar{1}$	.816	6.5	+5.8	143	.607	1.1	+0.6
$73\bar{2}$	.781	8.2	+7.5	142	.569	2.5	+4.2
$73\bar{3}$	.759	< 1.8	-3.4	141	.540	3.8	-4.8
$73\bar{4}$	.742	8.9	+7.5	140	.523	< 1.5	+1.7
$73\bar{5}$	.733	8.1	+8.6	$14\bar{1}$	.519	8.6	+9.9
$73\bar{6}$	.737	5.3	-6.2	$14\bar{2}$	.530	1.5	-3.7
$73\bar{7}$	.746	1.1	-1.0	$14\bar{3}$	.553	5.7	+6.1
$73\bar{8}$	.772	< 1.5	+0.2	$14\bar{4}$	.587	5.0	+6.1
$73\bar{9}$	.798	3.7	-4.5	$14\bar{5}$	.632	13.0	-13.8
$73\bar{10}$	.838	3.3	-3.9	$14\bar{6}$	.682	9.3	-6.5
$73\bar{11}$	.878	1.5	-1.5	$14\bar{7}$	.740	< 1.8	+0.2
$73\bar{12}$	.932	< 1.2	+0.1	$14\bar{8}$	.800	4.7	-5.3
$73\bar{13}$	.905	< 1.4	-1.2	$14\bar{9}$	.867	< 1.5	-1.0
830	.955	1.9	-1.2	$14\bar{10}$	.924	3.5	+2.9
$83\bar{1}$	.909	7.6	-5.8	248	.962	< 1.2	+1.9
$83\bar{2}$	.878	7.9	-5.5	247	.895	< 1.2	+0.3
$83\bar{3}$	.847	< 1.7	-0.5	246	.831	< 1.4	-0.6
$83\bar{4}$	.829	5.9	+4.0	245	.769	5.1	+5.3
$83\bar{5}$	.816	8.4	+6.8	244	.712	< 1.6	-2.0
$83\bar{6}$	.811	3.9	+2.6	243	.660	6.7	-7.2
$83\bar{7}$	.816	< 1.4	-0.4	242	.617	< 1.1	+1.0
$83\bar{8}$	.829	< 1.1	+0.8	241	.530	1.4	+0.7
$83\bar{9}$	.851	< 1.3	-0.8	240	.556	1.9	-1.8
$83\bar{10}$	.878	< 1.5	+1.0	$24\bar{1}$	.543	8.2	-8.1
$83\bar{11}$	.914	1.4	+1.8	$24\bar{2}$	.543	4.7	-6.5
$83\bar{12}$	.951	1.0	-1.0	$24\bar{3}$	.551	8.5	+9.1
$93\bar{2}$	.974	4.7	+5.6	$24\bar{4}$	.582	9.4	+8.8
$93\bar{3}$	.941	< 1.2	-0.2	$24\bar{5}$	.618	10.2	+10.0
$93\bar{4}$	.919	< 1.4	+0.3	$24\bar{6}$	.662	10.5	+10.7
$93\bar{5}$	.901	5.8	+5.7	$24\bar{7}$	.713	2.2	-3.0
$93\bar{6}$	.896	< 1.1	-1.0	$24\bar{8}$	.769	5.9	-5.3
$93\bar{7}$	.891	1.5	-1.2	$24\bar{9}$	.831	< 1.4	-0.9
$93\bar{8}$	.901	< 1.1	+1.8	$24\bar{10}$	.895	< 1.2	-0.7

hkl	sin θ	$F_{obs.}$	$F_{calc.}$	hkl	sin θ	$F_{obs.}$	$F_{calc.}$
$2,4,\bar{11}$	.966	< 0.8	+0.2	$54\bar{4}$	.678	9.8	+11.0
$34\bar{7}$	.966	< 0.7	-1.3	$54\bar{5}$	.688	6.4	+5.9
$34\bar{6}$	.904	< 1.0	+0.2	$54\bar{6}$	.706	4.4	-4.4
$34\bar{5}$	.839	< 1.2	-0.5	$54\bar{7}$	.733	< 2.1	+1.7
$34\bar{4}$	.781	3.2	+2.0	$54\bar{8}$	.766	< 1.4	-0.4
$34\bar{3}$	.726	5.8	+4.6	$54\bar{9}$	.812	1.9	-3.0
$34\bar{2}$	.679	2.7	+4.6	$5,4,\bar{10}$	.859	2.4	+2.3
$34\bar{1}$	.639	2.2	-3.9	$5,4,\bar{11}$	.912	< 1.2	0.0
340	.608	1.5	-0.1	$5,4,\bar{12}$	.962	< 1.4	-0.5
341	.586	10.0	+11.7	$64\bar{3}$	.970	< 1.0	-1.5
342	.577	2.6	+1.0	$64\bar{2}$	.920	< 1.2	+0.5
343	.580	5.0	+10.0	$64\bar{1}$	.871	< 2.2	-0.9
344	.596	15.1	+17.5	640	.835	< 3.0	-4.8
345	.622	3.6	-4.9	641	.796	< 0.9	-0.5
346	.658	8.8	-10.2	642	.769	1.6	-1.3
347	.702	< 1.3	+2.0	643	.751	< 1.5	-1.3
348	.755	3.7	-3.9	644	.744	8.3	+8.5
349	.807	3.5	-4.0	645	.744	3.2	+2.8
$3,4,\bar{10}$	.871	2.2	+2.2	646	.755	2.9	-4.4
$3,4,\bar{11}$	.932	< 0.9	-0.3	647	.773	< 1.4	+0.7
446	.979	< 1.3	-1.0	648	.80	< 2.0	+0.7
445	.916	2.7	-1.4	649	.835	< 1.3	-0.8
444	.855	3.1	-1.8	$6,4,\bar{10}$	.875	1.4	-1.4
443	.804	4.7	-4.5	$6,4,\bar{11}$	.920	1.8	-1.8
442	.755	< 1.7	-0.1	$6,4,\bar{12}$	.966	< 1.1	+0.9
441	.708	0.9	-0.6	741	.962	< 1.4	-1.4
440	.673	2.9	-3.5	740	.920	< 2.3	-1.9
$44\bar{1}$	.646	6.1	-4.6	$74\bar{1}$	.883	3.0	-1.9
$44\bar{2}$	.628	7.9	-8.6	$74\bar{2}$	.851	< 0.8	-0.3
$44\bar{3}$	.625	5.9	+5.3	$74\bar{3}$	.831	< 1.1	+0.1
$44\bar{4}$	.630	15.4	+15.2	$74\bar{4}$	.815	2.7	+1.6
$44\bar{5}$	.647	5.5	+4.9	$74\bar{5}$	.807	5.0	+4.1
$44\bar{6}$	.674	5.0	+3.3	$74\bar{6}$	.812	2.8	+2.1
$44\bar{7}$	.709	2.8	+1.5	$74\bar{7}$	.819	1.5	+2.0
$44\bar{8}$	.755	3.8	-3.5	$74\bar{8}$	.843	< 1.3	+0.1
$44\bar{9}$	.804	1.2	-1.0	$74\bar{9}$	.867	< 1.8	-1.4
$4,4,\bar{10}$	.859	< 0.9	0.0	$7,4,\bar{10}$	.904	3.1	+3.2
$4,4,\bar{11}$	.916	< 1.9	0.0	$7,4,\bar{11}$	.941	0.8	+1.4
$4,4,\bar{12}$	.983	< 1.0	-1.0	$7,4,\bar{12}$	.992	< 0.4	-0.1
544	.941	< 2.5	-2.3	$84\bar{1}$	.970	< 1.3	+0.2
543	.883	3.2	+2.5	$84\bar{2}$	.941	3.4	+4.3
542	.835	< 1.5	+2.3	$84\bar{3}$	.912	< 0.7	-0.7
541	.788	< 2.5	-1.0	$84\bar{4}$	.895	< 1.0	0.0
540	.751	3.0	-3.3	$84\bar{5}$	.883	2.3	+0.9
$54\bar{1}$	.715	3.4	+7.4	$84\bar{6}$	.879	4.7	-4.4
$54\bar{2}$	.694	4.3	+3.3	$84\bar{7}$	.883	< 1.2	-1.4
$54\bar{3}$	.682	3.5	+0.6	$84\bar{8}$	.895	< 0.9	+1.3

hkl	sin θ	$F_{obs.}$	$F_{calc.}$	hkl	sin θ	$F_{obs.}$	$F_{calc.}$
84$\bar{9}$	.916	< 1.0	-1.0	356	.982	< 0.6	-2.1
8,4,$\bar{10}$	.941	3.1	-2.1	355	.922	3.3	-2.5
8,4,$\bar{11}$	.975	2.5	-3.0	354	.870	1.6	-1.9
94$\bar{4}$	.979	< 0.4	-0.9	353	.821	< 1.3	+0.5
94$\bar{5}$	.962	< 1.6	-1.2	352	.780	1.2	-2.5
94$\bar{6}$	.958	< 0.9	+2.0	351	.745	4.3	-4.9
94$\bar{7}$	.953	3.4	+2.5	350	.718	2.0	-1.3
94$\bar{8}$	.962	< 0.8	-0.5	35$\bar{1}$	.701	3.2	-1.4
94$\bar{9}$	.975	1.4	-1.8	35$\bar{2}$	.693	2.1	-3.5
9,4,$\bar{10}$	.992	< 0.6	+2.0	35$\bar{3}$	.696	5.8	+6.9
158	.978	< 0.8	-2.0	35$\bar{4}$	.709	7.1	+6.6
157	.919	3.1	-2.6	35$\bar{5}$	.731	4.4	+3.6
156	.860	3.1	-1.0	35$\bar{6}$	.761	7.4	+8.7
155	.807	< 1.7	-0.9	35$\bar{7}$	.800	2.3	+2.2
154	.760	2.6	+0.6	35$\bar{8}$	.846	2.0	-2.5
153	.718	7.9	+7.4	35$\bar{9}$	.894	< 1.0	+0.7
152	.686	1.5	+1.0	3,5,$\bar{10}$	.952	1.2	-1.8
151	.663	3.3	-5.1	455	.993	< 1.2	-3.7
150	.649	< 1.7	+2.9	454	.937	< 1.6	-1.3
15$\bar{1}$	.646	1.2	-2.4	453	.890	2.2	+3.0
15$\bar{2}$	.654	< 1.5	-0.7	452	.846	< 1.5	+1.6
15$\bar{3}$	.673	11.3	+11.8	451	.438	4.6	-3.8
15$\bar{4}$	.702	8.2	+5.9	450	.775	4.1	-4.3
15$\bar{5}$	.739	4.5	+2.3	45$\bar{1}$	.751	3.7	+4.4
15$\bar{6}$	.783	3.5	+4.1	45$\bar{2}$	.736	3.8	+2.5
15$\bar{7}$	.833	2.3	-1.6	45$\bar{3}$	.733	2.8	+0.3
15$\bar{8}$	.887	2.8	-2.4	45$\bar{4}$	.738	7.5	+7.9
15$\bar{9}$	.948	< 1.1	-1.0	45$\bar{5}$	.752	3.9	-2.8
257	.974	< 0.8	+3.1	45$\bar{6}$	.775	10.3	-10.8
256	.915	1.6	-1.6	45$\bar{7}$	.806	< 1.5	+0.1
255	.860	4.7	-3.5	45$\bar{8}$	.846	< 1.1	+0.8
254	.809	2.8	-1.1	45$\bar{9}$	.890	0.7	-1.3
253	.763	2.3	-1.6	4,5,$\bar{10}$	.940	< 1.6	+1.4
252	.727	2.3	-0.3	4,5,$\bar{11}$	.993	< 1.0	+0.3
251	.696	2.9	-3.7	553	.963	< 1.3	-2.0
250	.676	2.1	-2.2	552	.919	1.7	-1.9
25$\bar{1}$	.665	< 1.6	+2.7	551	.877	2.1	-1.7
25$\bar{2}$	.665	< 1.6	-2.3	550	.843	3.6	-2.0
25$\bar{3}$	.676	9.1	+7.9	55$\bar{1}$	.812	3.9	-2.2
25$\bar{4}$	.697	10.1	+12.5	55$\bar{2}$	.793	4.0	-4.0
25$\bar{5}$	.727	6.5	-7.1	55$\bar{3}$	.782	< 1.9	-0.3
25$\bar{6}$	.765	7.0	-7.0	55$\bar{4}$	.780	< 1.5	+2.0
25$\bar{7}$	.810	< 1.5	+1.4	55$\bar{5}$	.788	1.7	+1.0
25$\bar{8}$	.860	2.7	-2.7	55$\bar{6}$	.803	7.1	+6.5
25$\bar{9}$	.915	< 1.1	-0.1	55$\bar{7}$	.827	4.7	+4.2
2,5,$\bar{10}$	.974	3.5	+3.1	55$\bar{8}$	.856	1.8	-2.8

hkl	sin θ	$F_{obs.}$	$F_{calc.}$	hkl	sin θ	$F_{obs.}$	$F_{calc.}$
$55\bar{9}$	.897	< 1.0	+0.8	$16\bar{6}$	.890	3.8	+3.2
$5,5,\bar{10}$	.940	5.8	+0.1	$16\bar{7}$	.935	< 1.2	+1.1
652	.997	< 1.7	+1.9	$16\bar{8}$	.983	< 0.8	-1.6
651	.952	< 1.6	-0.9	$26\bar{5}$	.959	3.2	-3.0
650	.919	< 2.3	-2.3	264	.914	< 1.2	+0.3
$65\bar{1}$	.883	< 0.8	+1.8	263	.873	7.5	+7.4
$65\bar{2}$	.860	4.9	+5.2	262	.841	3.0	+2.3
$65\bar{3}$	.843	< 1.3	-0.9	261	.815	4.8	-5.7
$65\bar{4}$	.837	2.6	+1.4	260	.798	2.0	+0.1
$65\bar{5}$	.837	< 1.4	-0.2	$26\bar{1}$	.789	< 1.5	+0.4
$65\bar{6}$	.846	3.9	-4.7	$26\bar{2}$	.789	1.7	-2.7
$65\bar{7}$	.863	2.8	-1.6	$26\bar{3}$	.798	2.6	+3.5
$65\bar{8}$	.887	< 1.6	+0.3	$26\bar{4}$	.816	2.0	+1.6
$65\bar{9}$	.919	1.0	-1.7	$26\bar{5}$	.842	< 1.5	-2.0
$6,5,\bar{10}$	.955	< 0.7	+0.3	$26\bar{6}$	.874	< 1.1	+0.5
$6,5,\bar{11}$	.997	< 0.3	-0.5	$26\bar{7}$	.914	1.6	-0.4
750	.997	< 0.8	+0.5	$26\bar{8}$	.959	< 0.9	-0.2
$75\bar{1}$	.963	< 1.4	-1.6	364	.968	< 0.7	+0.2
$75\bar{2}$	.933	2.7	-2.2	363	.924	3.8	-3.9
$75\bar{3}$	.915	2.9	-2.3	362	.888	4.4	-3.9
$75\bar{4}$	.901	3.1	-1.7	361	.858	1.8	-0.8
$75\bar{5}$	.894	2.2	-1.5	360	.834	1.2	-2.0
$75\bar{6}$	.897	1.6	+1.5	$36\bar{1}$	.819	< 1.2	+1.2
$75\bar{7}$	.904	2.1	+2.5	$36\bar{2}$	.813	< 1.3	+0.3
$75\bar{8}$	.926	1.4	-2.4	$36\bar{3}$	.815	< 1.5	+1.7
$75\bar{9}$	.948	2.2	-1.0	$36\bar{4}$	.826	< 1.2	+1.5
$7,5,\bar{10}$	.982	< 0.7	+0.8	$36\bar{5}$	.845	2.0	-1.2
$85\bar{3}$	.989	< 0.4	+0.9	$36\bar{6}$	.872	1.4	-1.8
$85\bar{4}$	.974		-3.5	$36\bar{7}$	.905	< 0.9	+0.5
$85\bar{5}$	.963	2.3	-1.8	$36\bar{8}$	.947	1.4	-1.3
$85\bar{6}$	.959	< 1.1	+1.0	$36\bar{9}$	.989	< 0.5	+0.2
$85\bar{7}$	.963	< 0.8	+0.3	463	.986	< 0.9	+1.7
$85\bar{8}$	.974	1.8	-1.3	462	.947	2.6	+2.0
$85\bar{9}$	.993	< 0.6	-2.6	461	.910	< 0.8	-0.8
166	.959	4.1	-3.7	460	.883	1.0	-0.5
165	.912	3.1	-1.7	$46\bar{1}$	.862	< 1.3	+1.0
164	.870	3.0	-1.3	$46\bar{2}$	.850	< 1.8	-1.0
163	.834	8.6	-6.9	$46\bar{3}$	.847	2.6	-1.2
162	.807	6.6	-4.5	$46\bar{4}$	.851	3.0	-2.5
161	.787	3.5	-2.6	$46\bar{5}$	.863	< 1.4	-0.5
160	.775	< 1.5	-1.2	$46\bar{6}$	.884	5.3	+5.1
$16\bar{1}$	.773	1.2	+2.3	$46\bar{7}$	.911	< 1.1	+0.9
$16\bar{2}$	.780	3.2	+1.6	$46\bar{8}$	.947	3.0	-2.4
$16\bar{3}$	.796	5.9	+4.6	$46\bar{9}$	.986	< 1.9	+0.7
$16\bar{4}$	.820	2.8	+3.0	561	.974	< 1.3	+2.0
$16\bar{5}$	.852	< 1.1	-0.4	560	.944	< 0.6	-0.1

hkl	sin θ	$F_{obs.}$	$F_{calc.}$	hkl	sin θ	$F_{obs.}$	$F_{calc.}$
$56\bar{1}$	.916	< 0.9	0.0	$17\bar{4}$	.940	< 1.0	+0.3
$56\bar{2}$	.899	< 1.1	+2.0	$17\bar{5}$	.969	1.6	-1.4
$56\bar{3}$	.890	3.2	-3.5	273	.988	3.2	-4.5
$56\bar{4}$	.888	3.4	-2.2	272	.959	4.1	-1.7
$56\bar{5}$	.895	1.6	-0.3	271	.936	< 1.5	+1.7
$56\bar{6}$	.908	4.4	-4.6	270	.921	< 1.2	-1.0
$56\bar{7}$	.929	5.5	-3.3	$27\bar{1}$	.913	1.5	+2.1
$56\bar{8}$	.955	2.4	-1.4	$27\bar{2}$	.914	< 1.2	+1.8
$56\bar{9}$	.993	< 0.4	-1.0	$27\bar{3}$	.921	2.1	-2.7
$66\bar{1}$	.980	< 1.2	-0.6	$27\bar{4}$	.937	1.9	-2.2
$66\bar{2}$	.959	1.9	-1.4	$27\bar{5}$	.960	1.2	+1.2
$66\bar{3}$	.944	3.2	-1.6	$27\bar{6}$	.989	2.9	+3.5
$66\bar{4}$	.938	5.1	-3.6	371	.974	< 1.3	+1.7
$66\bar{5}$	.938	< 1.0	-1.5	370	.953	< 0.8	+0.1
$66\bar{6}$	.947	3.8	+5.6	$37\bar{1}$	.940	< 0.9	+0.2
$66\bar{7}$	.962	2.8	+3.5	$37\bar{2}$	.934	3.0	-3.1
$66\bar{8}$	.983	3.1	-3.8	$37\bar{3}$	.936	3.6	-3.7
$76\bar{4}$	.996	< 0.5	-3.4	$37\bar{4}$	.946	1.8	-1.1
$76\bar{5}$	.989	< 0.9	-0.1	$37\bar{5}$	.963	< 0.8	-0.4
$76\bar{6}$	.993		-2.9	$37\bar{6}$	.986	2.7	-1.8
174	.985	< 0.8	+0.1	470	.996	< 0.8	+0.9
173	.953	2.3	+2.6	$47\bar{1}$	.978	< 0.7	-0.6
172	.929	< 1.0	+0.4	$47\bar{2}$	.967	1.6	+1.9
171	.912	1.5	-1.8	$47\bar{3}$	.965	2.2	-2.9
170	.902	1.9	+0.9	$47\bar{4}$	.968	1.5	-2.7
$17\bar{1}$	.900	1.8	-1.4	$47\bar{5}$	.979	< 1.3	+1.1
$17\bar{2}$	.906	4.4	-4.4	$47\bar{6}$	.997	< 1.5	+1.3
$17\bar{3}$	.919	2.5	-1.2				

THE CRYSTAL STRUCTURE OF TETRACENE.

Crystal Data.

Tetracene (naphthacene, 2,3 benzanthracene) $C_{18}H_{12}$; molecular weight 228.3; melting point 357°; Triclinic.

$a = 7.98A$ $b = 6.14A$ $c = 13.57A$

$\alpha = 98°03'$ $\beta = 112°24'$ $\gamma = 92°30'$

$a^* = 0.2099A$ $b^* = 0.2550A$ $c^* = 0.1246A$

$\angle(010):(001) = 78°48'$, $\angle(001):(100) = 66°54'$

$\angle(100):(010) = 83°44'$

Space group $P_{\bar{I}}$. Two molecules per unit cell. Molecular symmetry, centre. Volume of the unit cell = $605A^3$. Absorption co-efficient for X-rays ($\lambda = 1.54$) $\mu = 6.80$ per centimetre. Total number of electrons per unit cell = $F_{(000)} = 240$.

Experimental.

The crystals grown from xylene (Clar 1942), were in the form of orange red leaflets of extremely thin cross section. By recrystallisation from tetralin, very small, more evenly developed, specimens were obtained, but these showed an invariable tendency to twinning. The same effect was encountered in crystals obtained by slow sublimation at 170°C. The crystals were very friable, and attempts to separate the twins by mechanical means were therefore

unsuccessful. The plate-like crystals obtained from xylene, in which the (001) face only is well developed, were used for the preliminary investigation.

Determination of Crystal Constants.

Copper K_α radiation ($\lambda = 1.54A$) was used throughout this X-ray investigation. Rotation, oscillation, and Weissenberg moving film photographs taken about the axes and diagonals, gave the dimensions of the unit cell, and confirmed that tetracene belonged to the triclinic system. The values obtained for the axial lengths were in good agreement with previous results (Hertel and Bergk 1936).

Measurement of Intensities.

Reflections from the (hol) and (okl) zones were obtained by taking moving film exposures of the equatorial layer lines for crystals rotated about the a and b crystal axes. The multiple film technique (Robertson 1943) was used to obtain accurate correlation between very strong and very weak reflections, the integrated intensities being obtained by careful visual estimation.

For the (hol) zone the crystal employed had a cross-section normal to the b axis of 0.86 millimetre by 0.005 millimetre, and for the (okl) zone the crystal had a cross section of 0.81 millimetre by 0.005 millimetre normal

to the a axis.

The intensity range obtained in the six hour exposures normally employed, was not very large, and, in order to extend it twelve hour exposures were taken. This increased the range to 2000 to 1 on the (hol) zone and to 1500 to 1 on the (okl) zone. This length of exposure time was almost the maximum possible, as the background radiation appeared to be building up very rapidly.

Owing to the lack of uniformity in cross section of the crystals employed, it was thought that absorption corrections would be very important. However it was found that, due to the extreme thinness of the crystal specimens, the mean path through the crystal was almost constant for all planes, with the exception of six. Absorption corrections were therefore made for those planes, and all the intensities corrected for Lorenz and polarisation effects.

The values of the structure amplitudes finally derived are listed as F_{meas} in Table XVIII. Absolute measurements of intensities were not carried out, and the scale of the F values was obtained by correlation with the structure factors calculated from the atomic parameters.

Determination of the Space Group.

Since tetracene belongs to the triclinic system the space group must be either P_1 or $P_{\bar{1}}$, corresponding to

no symmetry, and to a centre of inversion respectively. X-ray diffraction effects give no means of distinguishing between these two space groups, but it was hoped that a test for the pyro-electric effect would indicate whether the crystal was polar or non-polar.

This effect depends on the principle that non-centro symmetric crystals when heated or cooled quickly develop equal and opposite charges at either end of the polar axis, and this change is detectable by the adhesion of the crystal to a metal plate placed in the cooling agent.

It was found, however, that all the crystals used in the experiment whether polar or non-polar, gave a positive result for this test, probably due to a surface tension phenomenon. An attempt was therefore made to determine the space group on the basis of a close similarity to the anthracene structure.

It is rather interesting that there should be a change in the crystal system from monoclinic to triclinic in passing from anthracene to tetracene. The change involved in molecular structure here, is precisely the same as that between naphthalene and anthracene, which are crystallographically very alike, and show the gradation in properties expected from a homologous series. A comparison

of the axial lengths of the three compounds, however, reveals quite definite similarities (Table XII). To make this comparison possible, the usual convention in naming the axes of triclinic crystals has not been employed.

Table XII.

Comparison of unit cell dimensions in naphthalene, anthracene and tetracene.

	a	b	c	β
Naphthalene	8.24A	6.00A	8.66A	122.9°
Anthracene	8.56	6.04	11.16	124.7
Tetracene	7.98	6.14	13.57	112.4

The a axis shows a slight variation, due to a slightly different tilt of the molecule. The b axis remains practically constant in the three compounds, whereas the c axis, which increases by 2.5A in going from naphthalene to anthracene to accommodate the extra ring, increases by 2.4A in going from anthracene to tetracene. This appeared to indicate that the long axis of the molecule in tetracene lay close to the c axis as in naphthalene and anthracene, and that the increase in length was due to the greater longitudinal extensions of the four ring system.

Extending the analogy to the values of the angles

the similarity is again revealed by the fact that the α and γ angles in tetracene are almost right angles.

A comparison of melting points also showed the smooth gradation expected from a homologous series.

Naphthalene	80°C
Anthracene	217°C
Tetracene	357°C

It seemed apparent therefore, that the arrangement of the molecules in the crystal lattice of tetracene would be closely analogous to the arrangement in the anthracene lattice without, however, maintaining the monoclinic symmetry.

In anthracene the arrangement of the molecules in the projection along the c axis is as shown in Fig. 19.

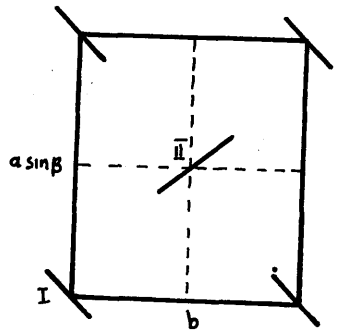

Fig. 19. Diagram of the projection along the c axis in anthracene.

Molecule I reproduces itself at the centre of the unit cell, by virtue of the "a" glide plane. This symmetry

gives rise to halvings in the (hol) zone ((hol) absent when h is odd). In tetracene, although (101) and (301) spectra are present, they are extremely weak in comparison with (201) planes. This fact, therefore, suggests that, although the central molecule in tetracene is not related by any symmetry elements to molecule I, it lies very close to such a position. Thus there are two unrelated molecules in the unit cell, which conforms to the P_1 space group.

The tetracene molecule, however, possesses a centre of symmetry which may or may not be used in forming the structure. If we assume that it is used, and place it at the origin and centre in Fig. 19, we have an arrangement in the unit cell bearing an even closer resemblance to the anthracene structure. This is the $P_{\bar{1}}$ space group with pseudo $P2_{1/a}$ symmetry, thus giving the greatest possible similarity to the two preceding homologous hydrocarbons.

It therefore seemed logical to accept this space group of higher symmetry for at least the first trial structure.

Analysis of the Structure.

A comparison of Weissenberg moving films of anthracene and tetracene showed a marked similarity in the intensities of corresponding reflections. Two of the strongest

planes observed in naphthalene and anthracene were the (200) and (20$\bar{1}$) planes and this was also the case in tetracene. Also the relative values of the intensities along the c axis showed a close relation in the three compounds.

This suggested that the structure given by the projection along the b axis would be similar to anthracene and naphthalene. A trial model was therefore set up, having the same tilt as the anthracene molecule with respect to the (010) plane.

This model automatically gave rise to halvings in the (hol) structure factors. After several adjustments had been made in the orientations of the two half molecules, in an attempt to increase the structure amplitudes of these planes, a set of atomic co-ordinates was found which gave some measure of agreement between the observed and calculated values of the structure factors. The discrepancy for all the observed planes was 36.4%. and a Fourier synthesis was therefore carried out. The resulting contour map did not give sharp definition of the atomic positions, and showed odd unevenness in contour distribution. On recalculating the structure factors from the revised co-ordinates, it was observed that the discrepancy was substantially unaltered, and that no significant sign changes had occurred. From this

it was deduced that the trial structure was wrong but that the general positions of the molecules were probably fairly accurate.

In this trial structure the apparent angle which the long axis of the molecule made with the a axis was 105° compared with 120° in anthracene and 116° in naphthalene. Due to this variation it was thought likely that the orientation with respect to the (010) plane might also differ considerably from that of anthracene. The number of possibilities with two unrelated molecules was so great that to exhaust all of them by trial and error methods would have been extremely tedious.

Attention was therefore directed to the projection along the a axis, as this projection would be more sensitive to small variations in the tilt of the molecules from the (010) plane. An approximate orientation was taken from the best trial structure in the first projection, and adjusted to secure agreement between the observed and calculated structure factors. Atomic co-ordinates were found which gave a discrepancy of 32.9% over all the observed planes. A Fourier summation on the basis of these positions was carried out, and on recalculating the structure factors the discrepancy from the measured values was found to be 27.8%

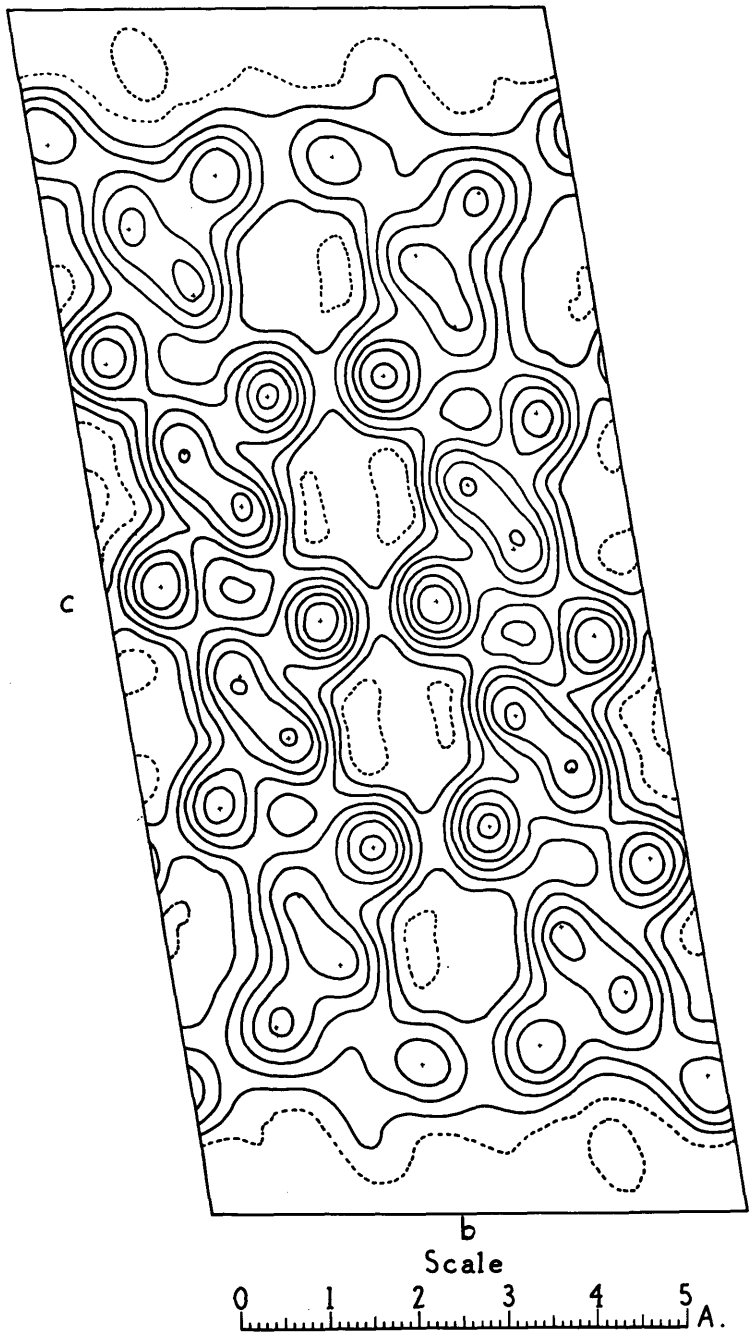

Fig. 20. Projection of the tetracene structure along the a crystal axis, drawn on the (100) plane. Each contour line represents a density increment of one electron per A^2, the one electron line being dotted.

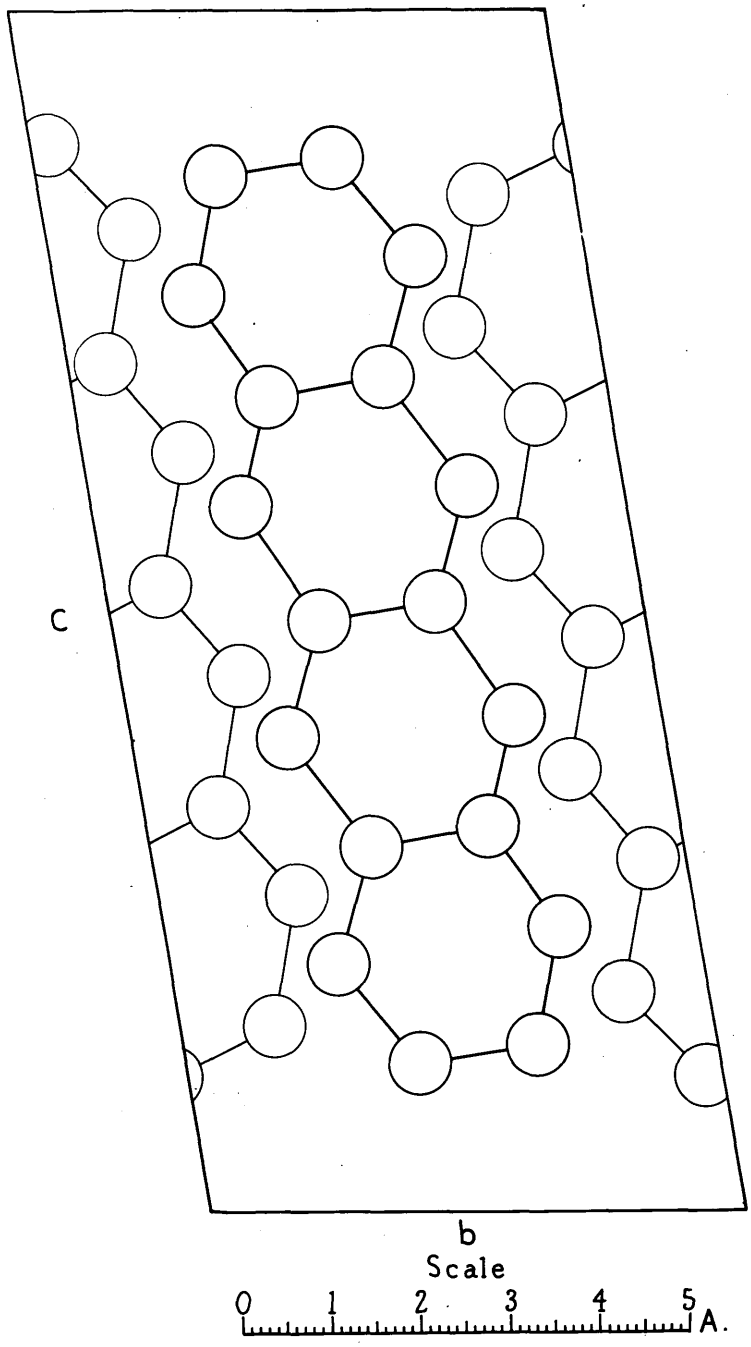

Fig. 21. Arrangement of the molecules in the a axis projection.

A second Fourier reduced this discrepancy to 21%. Since only one plane had changed sign the structure did not seem to warrant any further refinement.

The summation of the electron series

$$\rho(y,z) = \frac{1}{A}\sum_{-\infty}^{+\infty}\sum_{-\infty}^{+\infty} F_{(okl)} \cos 2\pi\left(\frac{ky}{b} + \frac{lz}{c}\right)$$

was carried out by a three figure stencil method (Robertson 1948). The b and c axes were divided into 30 and 60 parts respectively, the intervals along b being 0.205Å and along the c axis 0.226Å. The series was calculated over half the unit cell, and the results are represented by the contour map of Fig. 20, where the contour lines drawn at unit electron intervals were obtained by graphical interpolation from the summation totals. Since the F values are not really absolute the density increments are only approximately one electron per line, and the peak values are actually somewhat higher than expected from a structure of this kind. These considerations, however, have no effect on the atomic positions. This projection has been drawn on the (100) plane. Although this plane is not normal to the a axis, as is customary, the deviation is not sufficient to distort the atoms, and does not affect the derived co-ordinates.

This projection gave reliable values for the y

and z co-ordinates of the atoms. Using the z co-ordinates and the orientation calculated from this projection, approximate co-ordinates were obtained for the projection along the b axis. These were very similar to those of the first trial structure in this projection, except in the respect that the second molecule was reversed from the previous position. Much better agreement was obtained between the measured and calculated structure factors, and the discrepancy for the observed planes was 23.5%.

Using the phases calculated from this structure a summation of the electron density series

$$\rho(x,z) = \frac{1}{A}\sum_{-\infty}^{+\infty}\sum_{-\infty}^{+\infty} F_{(hol)} \cos 2\pi \left(\frac{hx}{a} + \frac{lz}{c} \right)$$

was carried out. Fig. 22 shows the contour map obtained, and the explanatory diagram is shown in Fig. 23.

This projection has been drawn on a plane normal to the b crystal axis. Since the axes are triclinic, this projection plane does not coincide with any crystal plane, but is inclined at an angle of 10° to (010). The sides of this projection plane are $a\sin\gamma$ and $c\sin\alpha$, and the angle between them β^* is 113°06'. $a\sin\gamma$ was divided into 30 parts, giving an interval of 0.266A, and $c\sin\alpha$ was divided into 60 parts giving an interval of 0.223A.

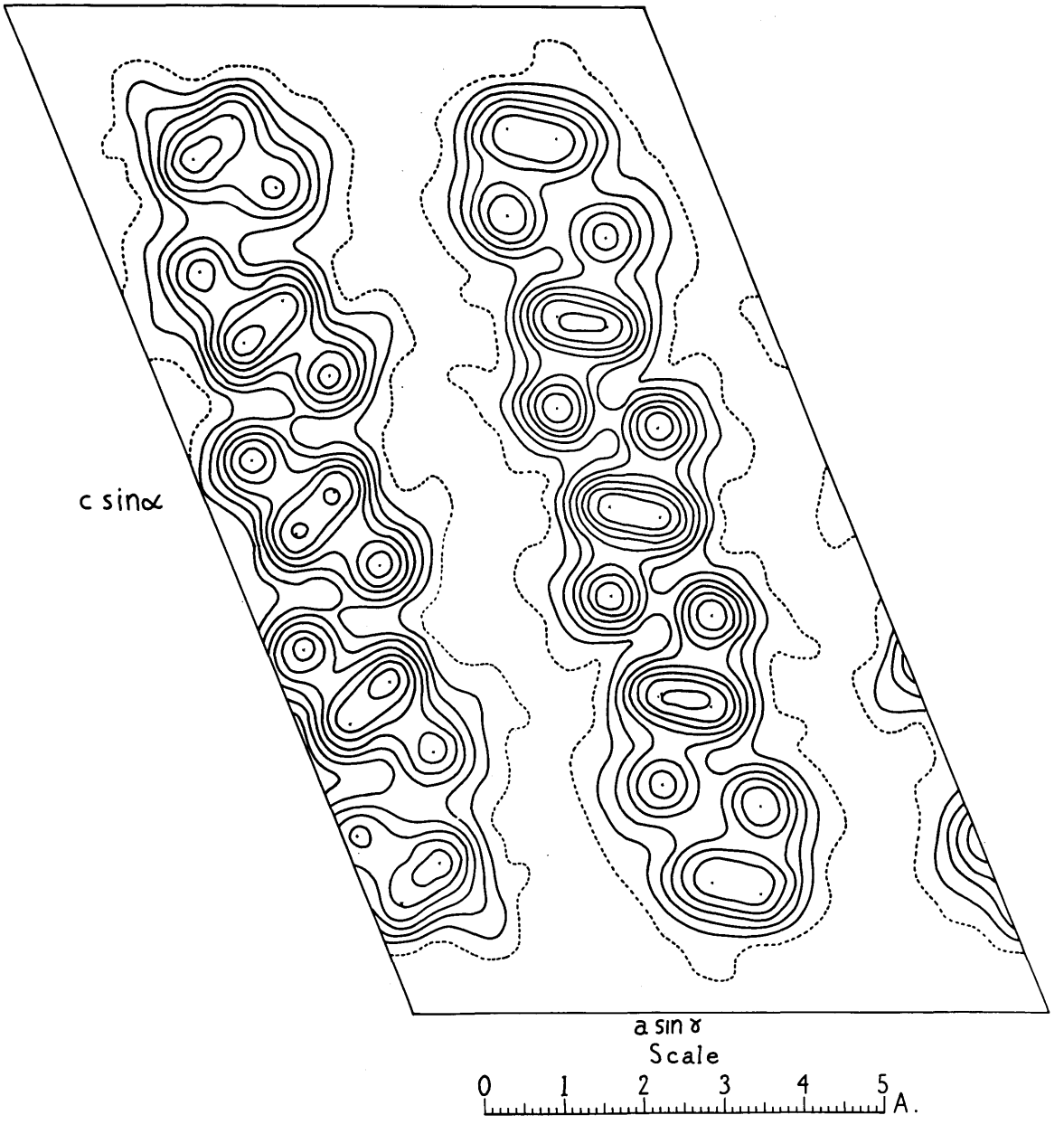

Fig. 22. Normal projection of the tetracene structure along the b crystal axis. Each contour line represents a density increment of one electron per A^2, the one electron line being dotted.

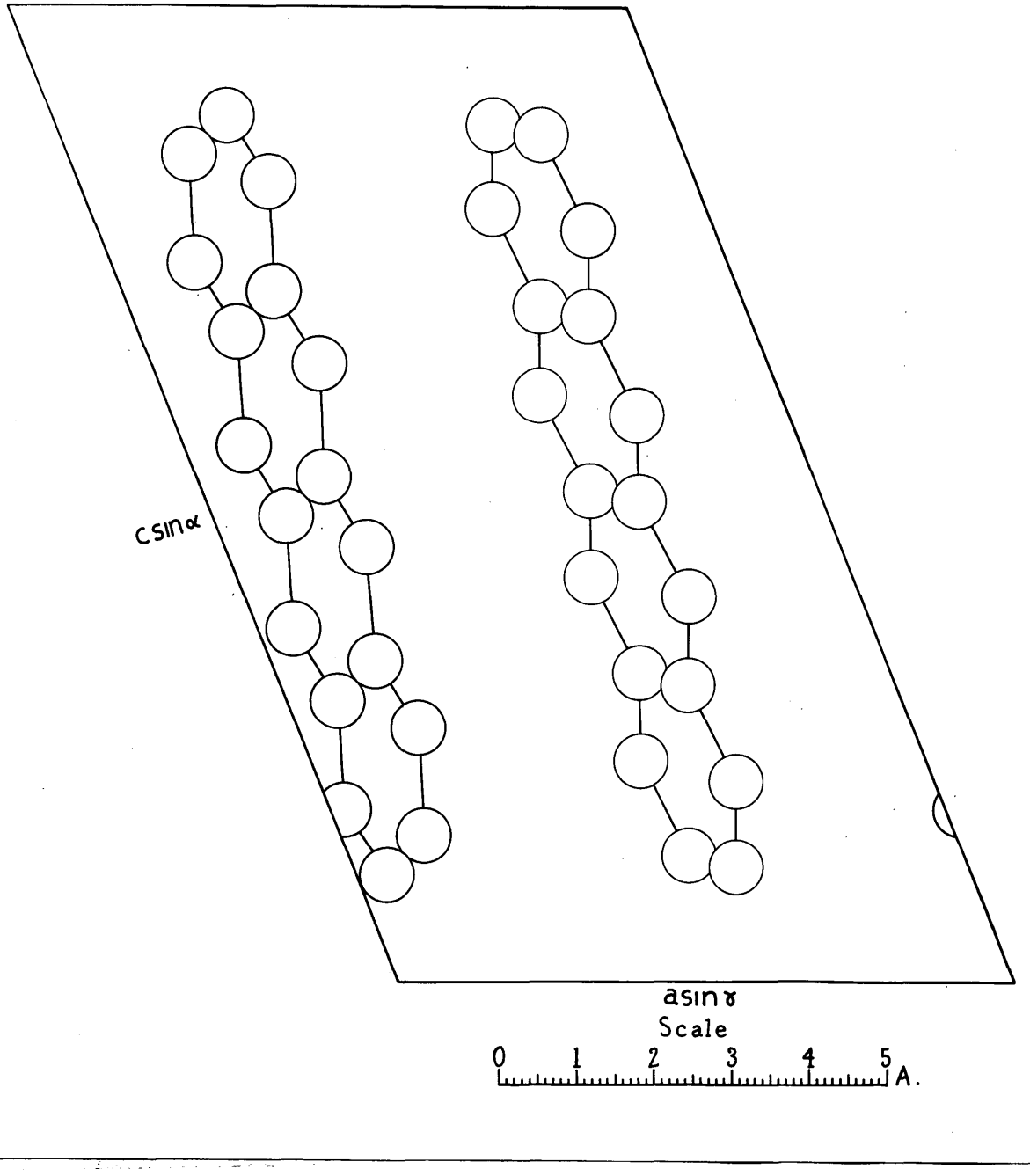

Fig. 23. Arrangement of the molecules in the b axis projection.

The electron density distribution obtained by graphical interpolation of these results is very similar to the analogous projection of anthracene (Fig. 1).

Co-ordinates, Dimensions and Orientation.

The projection along the a axis shows the two half molecules comprising the asymmetric unit. The molecules overlap slightly in projection, but in space the second molecule is situated half a translation along the a axis from the first one.

Of the eighteen atoms comprising the asymmetric unit, the ten forming the inner pairs are separately resolved, but the exact positions of the others are obscured by the overlap. The arrangement is shown in Fig. 21.

Although the planes of the molecules are inclined at an angle of 60° to the plane of projection, in the projection along the b axis, yet good resolution of the atoms has been obtained. In this projection the second molecule is situated half a translation along the b axis from the first one, and the outer pairs of atoms are separately resolved, and standing out clearly as isolated peaks.

Thus, by combining the a and b axis projections a separate picture is obtained of every atom in the

Table XIII.

Co-ordinates in Angstrom units referred to triclinic crystal axes; centre of symmetry as origin.

	xA	yA	From a projection zA	From b projection zA
C_1	0.95	0.20	5.24	5.24
C_2	1.14	0.94	4.30	4.30
C_3	0.65	0.44	2.78	2.82
C_4	0.85	1.16	1.81	1.82
C_5	0.35	0.62	0.29	0.28
C_6	-0.54	-1.37	0.70	0.70
C_7	-0.04	-0.84	2.21	2.26
C_8	-0.24	-1.59	3.17	3.20
C_9	0.26	-1.08	4.68	4.68
C'_1	4.33	3.43	5.10	5.10
C'_2	3.88	4.17	3.97	3.95
C'_3	4.01	3.57	2.63	2.60
C'_4	3.55	4.28	1.46	1.38
C'_5	3.70	3.75	0.11	0.07
C'_6	4.71	1.73	1.05	1.12
C'_7	4.58	2.23	2.41	2.46
C'_8	5.01	1.60	3.91	3.66
C'_9	4.89	2.08	4.89	4.96

asymmetric unit.

The co-ordinates obtained from these electron density maps are shown in Table XIII.

Thirty six of the fifty four parameters could be measured directly on the diagrams, and the estimated centres of the other atoms were consistent with a planar molecule containing regular hexagon rings. The z co-ordinates were estimated separately on both the (hol) and (okl) projections and are in fairly good agreement. The co-ordinates obtained from the projection along the a axis are probably the more reliable as further refinement is necessary in the (hol) projection.

In Table XIV the co-ordinates are expressed as fractions of the axial lengths in degrees.

From these parameters the structure factors were recalculated, and a comparison with the measured values is given in Table XVIII. The overall discrepancy is rather higher than that found in the anthracene structure determination. There are two main reasons for this. The first is the very large number of planes with small geometrical structure factors, caused by the pseudo-monoclinic symmetry of the structure, and the second is the limitation of the observed range of intensities, due to the rather unsuitable nature of the crystal specimens employed.

Table XIV.

Co-ordinates in degrees.

	$\frac{2\pi x}{a}$	$\frac{2\pi y}{b}$	$\frac{2\pi z}{c}$
C_1	43.0°	11.9°	140.0°
C_2	51.5	56.1	115.0
C_3	29.4	26.3	74.2
C_4	38.5	69.4	48.3
C_5	15.8	37.1	7.7
C_6	-24.4	-82.0	18.7
C_7	-1.8	-50.2	59.0
C_8	-10.8	-95.0	84.6
C_9	11.7	-64.5	125.0
C'_1	195.4	201.5	136.1
C'_2	175.0	245.6	106.0
C'_3	180.9	210.2	70.3
C'_4	160.2	250.4	39.0
C'_5	166.9	221.0	2.9
C'_6	212.5	100.0	28.0
C'_7	206.5	129.9	64.4
C'_8	226.0	92.1	94.7
C'_9	220.7	120.9	130.8

As the structure has not yet been completely refined, no measurements have been made of exact inter-atomic distances, but the co-ordinates so far obtained are in harmony with a planar molecule composed of regular hexagon rings, and an inter-atomic distance of about 1.40A. Further refinement may, however, indicate small variations in these bond lengths.

The orientation of the molecule is most conveniently referred to an orthogonal system of axes. For this purpose arbitrary axes were chosen, consisting of the b crystal axis, the projected a axis (asinγ), and another axis c' perpendicular to this axis, and lying in the plane of projection normal to the b axis. The orientation of the molecules with respect to these three axes is given in Table XV. The long axis of the molecule is denoted by L, the short cross axis by M, and the axis at right angles to both of these by N. The angles between these molecular axes and the orthogonal axes are shown as χ_L, ψ_L, ω_L, etc.

These may be compared with the orientation of anthracene (Robertson 1933), referred to analogous orthogonal axes, given in Table XVI.

From the orientations of the two molecules comprising the asymmetric unit in tetracene, it can be seen that they are almost related by a screw axis.

Table XV.

Orientation of molecular axes in tetracene.

Molecule I		Molecule II	
$\chi_L = 104.8°$	$\cos\chi_L = -0.255$	$\chi_L = 105.3°$	$\cos\chi_L = -0.264$
$\psi_L = 107.0$	$\cos\psi_L = -0.292$	$\psi_L = 99.3$	$\cos\psi_L = -0.161$
$\omega_L = 22.9$	$\cos\omega_L = +0.922$	$\omega_L = 18.0$	$\cos\omega_L = +0.951$
$\chi_M = 70.1$	$\cos\chi_M = +0.341$	$\chi_M = 116.3$	$\cos\chi_M = -0.444$
$\psi_M = 30.2$	$\cos\psi_M = +0.864$	$\psi_M = 27.0$	$\cos\psi_M = +0.891$
$\omega_M = 68.2$	$\cos\omega_M = +0.371$	$\omega_M = 84.6$	$\cos\omega_M = +0.094$
$\chi_N = 25.3$	$\cos\chi_N = +0.904$	$\chi_N = 30.2$	$\cos\chi_N = +0.865$
$\psi_N = 114.2$	$\cos\psi_N = -0.409$	$\psi_N = 66.6$	$\cos\psi_N = +0.398$
$\omega_N = 83.1$	$\cos\omega_N = +0.121$	$\omega_N = 72.1$	$\cos\omega_N = +0.307$

Table XVI.

Orientation of molecular axes in anthracene.

$\chi_L = 119.7°$	$\cos\chi_L = -0.495$
$\psi_L = 96.9$	$\cos\psi_L = -0.121$
$\omega_L = 30.7$	$\cos\omega_L = +0.860$
$\chi_M = 69.6$	$\cos\chi_M = +0.349$
$\psi_M = 28.6$	$\cos\psi_M = +0.878$
$\omega_M = 70.9$	$\cos\omega_M = +0.327$

The angles which the triclinic crystal axes make with the orthogonal reference axes are shown in Table XVII.

Table XVII.

Orientation of triclinic crystal axes in tetracene.

$\chi_a = 2.5°$	$\chi_b = 90.0°$	$\chi_c = 67.8°$
$\psi_a = 92.5$	$\psi_b = 0.0$	$\psi_c = 98.1$
$\omega_a = 90.0$	$\omega_b = 90.0$	$\omega_c = 23.9$

Electron Distribution.

A noticeable feature of the contour maps (Figs. 20 and 22) is that there is a slight falling off in the peak values of the electron density in the end benzene rings. this corresponds, to a lesser extent, to the effect found in anthracene, which was also detectable by a two dimensional structure determination (Robertson 1933). The fact that this decreasing electron density on the outer atoms of the molecules has been observed in both anthracene and tetracene tends to confirm the view that it is caused by some kind of thermal agitation.

Discussion.

The most interesting feature of this structure determination is the close similarity of tetracene to the two preceding hydrocarbons. Although there are definite variations in orientation, the general arrangement of the molecules in the unit cell is very like that of anthracene. It is therefore surprising that the crystal system should

change from monoclinic to triclinic in passing from anthracene to tetracene, and also that the appearance of the crystals should change so strikingly from colourless to bright orange red.

The first phenomenon cannot be fully discussed at this stage of the analysis, and will require to await further refinement of the atomic co-ordinates. The crystal system of a substance is determined by the packing of the molecules, and the arrangement which gives the lowest lattice energy will be the one normally adopted. A comparison of the closest approach distances between molecules, in anthracene and tetracene, should therefore provide an explanation of this change in symmetry.

A similar phenomenon was encountered in hexamethylbenzene (Brockway and Robertson 1939). In this compound the (001) plane approaches very closely to hexagonal symmetry ($a = 8.92A$, $b = 8.86A$, $\gamma = 119^\circ 34'$), and it was shown that this slight deviation resulted in a very much closer packing of the molecules in the crystal lattice, and an increase in density of 9%. The slight departure from monoclinic symmetry in tetracene will probably have a similar explanation.

Some elucidation of the remarkable change in colour

can be obtained from spectroscopic studies of naphthalene, anthracene and tetracene.

The investigation of the absorption spectra of the three substances in solution emphasises their close similarity in structure. It has been shown (Clar 1932, Seshan 1936) that the band spectrum becomes more diffuse on passing from naphthalene to tetracene, and shifts continuously towards the red end of the spectrum. The shift from naphthalene to anthracene is about 4970 $cm.^{-1}$ and from anthracene to tetracene 5230 $cm.^{-1}$.

These studies also show that there is a slight shift towards the red end of the spectrum in passing from the vapour state to solution, and again in passing from solution to the crystalline state. In tetracene and anthracene this shift is in the region of 200A. The first band of tetracene in solution is at 4680A, and in the solid at 4850A.

A noticeable feature, however, of the absorption spectrum of crystalline tetracene is the presence of another band at 5250A (Schiebe, Muller and Schiffmann 1941) which is completely absent in the vapour and solution states. This additional band accounts for the fact that the crystals of tetracene are bright red in colour, whilst the solution is pale yellow.

Similar bands are observed in the higher members of the series, pentacene and hexacene, but are completely absent in naphthalene and anthracene. It has been suggested that the appearance of this band in tetracene may be due to an arrangement whereby the molecules are more nearly parallel than in the anthracene structure, and some form of coupling can take place in the direction parallel to the N axis of the molecule. No evidence in support of this theory has, however, been given by the crystal structure as so far elucidated.

Spectroscopic studies have also been made of the absorption spectra of anthracene in the solid state, containing small amounts of tetracene as impurity (Krishnan and Seshan 1934). These investigations indicate that the tetracene molecules have some regular orientation in the anthracene crystal lattice, due to a form of "syncrystallisation" (Gaubert 1905), and take up positions nearly parallel to the anthracene molecules.

Recently a more detailed study of the fluorescence spectra of anthracene in solid solution containing small traces of tetracene has been made by Ganguly (1945), and by Bowen and Mikiewicz (1947). These investigations show that addition of small traces of tetracene greatly reduces the blue fluorescence of anthracene and gives rise to a strong

green fluorescence. A solid solution containing 1 mole tetracene to 10^4 moles anthracene fluoresced with the characteristic green colour of tetracene when excited by light of a wavelength which is mainly absorbed by anthracene (3650A) and this effect completely disappeared on dissolving the solid solution in benzene.

The suggested explanation of this phenomenon (Bowen 1945) is that the anthracene molecules absorb the light and pass the excitation energy through the crystal until it is captured by a tetracene molecule which then fluoresces. This theory would necessitate an extremely close resemblance in the crystal structures of anthracene and tetracene, and whether the similarity shown to exist by the present structure determination is sufficient to substantiate this hypothesis is a matter for conjecture.

Table XVIII.

Measured and Calculated Values of the Tetracene Structure Factors.

hkl	2sinθ	F meas.	F calc.	hkl	2sinθ	F meas.	F calc.
100	0.21	<1.3	-0.7	019	1.19	<4.8	+1.1
200	0.42	86.1	+94.3	018	1.07	<4.4	-2.7
300	0.63	<2.4	-2.0	017	0.95	<4.1	+3.3
400	0.84	3.7	+2.8	016	0.83	<3.7	+4.1
500	1.06	<3.5	-0.4	015	0.72	<3.4	+2.8
600	1.27	<3.9	-1.5	014	0.61	<3.0	-0.4
700	1.48	<4.0	+0.1	013	0.49	<2.7	-0.8
800	1.69	<3.6	+2.0	012	0.40	<2.4	+2.7
010	0.27	<1.9	+2.4	01$\bar{1}$	0.31	<2.0	-0.1
020	0.52	43.1	-36.2	01$\bar{1}$	0.27	3.4	-1.9
030	0.78	6.1	+6.1	01$\bar{2}$	0.33	<2.1	-0.4
040	1.04	8.7	-4.5	01$\bar{3}$	0.42	3.0	+2.4
050	1.30	<5.0	-0.3	01$\bar{4}$	0.52	3.0	-2.9
060	1.57	<4.9	-1.1	01$\bar{5}$	0.63	11.8	-5.6
070	1.83	<3.6	+1.6	01$\bar{6}$	0.75	3.4	-1.2
001	0.13	40.7	+39.7	01$\bar{7}$	0.87	<3.8	+0.8
002	0.25	33.6	-31.0	01$\bar{8}$	0.98	<4.2	-0.1
003	0.38	24.4	+21.3	01$\bar{9}$	1.10	<4.5	+1.1
004	0.50	16.3	-14.0	0,1,$\overline{10}$	1.23	4.6	-5.5
005	0.63	18.9	+19.4	0,1,$\overline{11}$	1.35	7.2	-7.7
006	0.75	13.8	+13.2	0,1,$\overline{12}$	1.47	<5.0	-0.5
007	0.88	5.1	-8.3	0,1,$\overline{13}$	1.59	<4.8	+1.2
008	0.99	<3.4	+4.8	0,1,$\overline{14}$	1.72	<4.3	-1.7
009	1.11	3.7	-2.5	0,1,$\overline{15}$	1.84	<3.6	+1.6
0,0,10	1.26	6.8	+3.1				
0,0,11	1.38	8.0	+4.1	0,2,14	1.89	<3.2	-1.2
0,0,12	1.48	<4.0	-1.6	0,2,13	1.77	<4.0	+1.3
0,0,13	1.60	<3.8	+0.9	0,2,12	1.66	<4.6	-1.3
0,0,14	1.72	<3.4	-0.4	0,2,11	1.54	7.2	-8.0
0,0,15	1.84	<2.8	+0.3	0,2,10	1.42	<5.1	-1.1
				029	1.31	<5.0	+0.8
0,1,14	1.79	<3.9	+0.1	028	1.20	<4.8	-1.2
0,1,13	1.67	<4.5	-0.4	027	1.09	<4.5	-1.7
0,1,12	1.55	<4.9	-0.1	026	0.98	5.9	+10.8
0,1,11	1.42	5,1	-4.6	025	0.88	17.3	+23.0
0,1,10	1.30	<5.0	+1.1	024	0.79	<3.6	-6.5

hkl	2sinθ	F meas.	F calc.
023	0.70	< 3.3	-0.3
022	0.62	9.3	+15.2
021	0.56	28.5	-32.0
02$\bar{1}$	0.51	3.8	-6.0
02$\bar{2}$	0.54	8.4	+10.6
02$\bar{3}$	0.58	8.9	-9.0
02$\bar{4}$	0.65	5.5	+4.4
02$\bar{5}$	0.73	38.5	+41.3
02$\bar{6}$	0.83	6.3	+6.8
02$\bar{7}$	0.93	< 4.0	-4.0
02$\bar{8}$	1.03	< 4.3	+2.5
02$\bar{9}$	1.14	< 4.6	-13.6
0,2,$\bar{10}$	1.25	12.7	+18.8
0,2,$\bar{11}$	1.37	7.2	+14.2
0,2,$\bar{12}$	1.48	< 5.0	-2.5
0,2,$\bar{13}$	1.60	< 4.8	+0.9
0,2,$\bar{14}$	1.72	< 4.3	-0.4
0,2,$\bar{15}$	1.84	< 3.6	+0.4
0,3,13	1.90	< 3.1	+0.4
0,3,12	1.79	< 3.9	-0.1
0,3,11	1.68	< 4.5	+1.3
0,3,10	1.58	< 4.8	+0.4
039	1.47	< 5.0	+0.7
038	1.37	< 5.1	+3.2
037	1.27	< 4.9	-4.3
036	1.17	11.8	-12.0
035	1.08	< 4.5	-1.6
034	1.01	< 4.3	+1.1
033	0.93	< 4.0	+0.7
032	0.87	< 3.8	-0.5
03$\bar{1}$	0.82	6.3	-2.1
03$\bar{1}$	0.77	< 3.5	+2.4
03$\bar{2}$	0.77	< 3.5	-0.5
03$\bar{3}$	0.80	< 3.6	-0.9
03$\bar{4}$	0.84	5.1	+6.6
03$\bar{5}$	0.90	12.3	+10.0
03$\bar{6}$	0.97	< 4.1	-3.2
03$\bar{7}$	1.05	< 4.4	+2.1
03$\bar{8}$	1.14	< 4.6	+0.1
03$\bar{9}$	1.23	< 4.9	-2.0
0,3,$\bar{10}$	1.33	12.7	+14.9
0,3,$\bar{11}$	1.44	6.3	+8.5
0,3,$\bar{12}$	1.54	< 4.9	-2.8
0,3,$\bar{13}$	1.65	< 4.6	+0.8
0,3,$\bar{14}$	1.76	< 4.1	-0.9
0,3,$\bar{15}$	1.87	< 3.3	-2.1
0,4,11	1.86	< 3.4	-3.7
0,4,10	1.76	< 4.1	+1.8
049	1.66	< 4.6	-2.7
048	1.56	< 4.9	+3.6
047	1.48	6.3	-4.8
046	1.39	27.9	-26.1
045	1.31	8.9	-5.7
044	1.24	<4.9	+4.4
043	1.18	<4.7	-9.6
042	1.12	<4.6	+2.4
04$\bar{1}$	1.08	8.9	-4.0
04$\bar{1}$	1.02	< 4.3	+5.6
04$\bar{2}$	1.02	< 4.3	-6.4
04$\bar{3}$	1.04	< 4.4	+6.2
04$\bar{4}$	1.07	4.6	-5.5
04$\bar{5}$	1.11	11.0	-11.3
04$\bar{6}$	1.16	< 4.7	+2.3
04$\bar{7}$	1.22	< 4.8	-0.8
04$\bar{8}$	1.29	< 5.0	+3.2
04$\bar{9}$	1.37	< 5.1	-1.5
0,4,$\bar{10}$	1.45	< 5.1	-11.3
0,4,$\bar{11}$	1.54	< 4.9	-3.3
0,4,$\bar{12}$	1.64	< 4.7	+1.6
0,4,$\bar{13}$	1.74	< 4.2	-0.3
0,4,$\bar{14}$	1.84	< 3.6	-0.5
059	1.86	< 3.4	+0.1
058	1.78	< 3.9	-1.1
057	1.69	< 4.4	+1.3
056	1.62	6.8	+4.1
055	1.55	< 4.9	+1.6
054	1.48	< 5.0	-3.7
053	1.42	< 5.1	-2.9
052	1.37	< 5.1	+0.1
05$\bar{1}$	1.33	< 5.0	-0.7
05$\bar{1}$	1.29	< 5.0	-2.7

hkl	2sinθ	F meas.	F calc.
$05\bar{2}$	1.28	< 5.0	+2.4
$05\bar{3}$	1.29	< 5.0	-1.1
$05\bar{4}$	1.30	< 5.0	-3.1
$05\bar{5}$	1.33	8.0	+6.6
$05\bar{6}$	1.37	< 5.1	+0.9
$05\bar{7}$	1.42	< 5.1	-1.9
$05\bar{8}$	1.47	< 5.0	+1.4
$05\bar{9}$	1.54	< 4.9	-1.6
$0,5,\overline{10}$	1.61	< 4.8	-2.8
$0,5,\overline{11}$	1.69	< 4.5	-0.3
$0,5,\overline{12}$	1.77	< 4.0	+2.0
$0,5,\overline{13}$	1.86	< 3.4	+0.1
066	1.85	< 3.5	+4.0
065	1.79	< 3.9	+0.1
064	1.73	< 4.3	-1.1
063	1.68	< 4.5	+1.6
062	1.64	< 4.7	-1.6
$06\bar{1}$	1.60	7.0	-8.0
$06\bar{1}$	1.55	< 4.9	+0.4
$06\bar{2}$	1.54	< 4.9	+1.2
$06\bar{3}$	1.54	< 4.9	+1.5
$06\bar{4}$	1.55	15.4	-12.1
$06\bar{5}$	1.57	8.4	-9.4
$06\bar{6}$	1.60	< 4.8	+3.5
$06\bar{7}$	1.64	< 4.7	-1.1
$06\bar{8}$	1.68	< 4.5	+0.5
$06\bar{9}$	1.73	< 4.3	-0.1
$0,6,\overline{10}$	1.79	< 3.9	-2.4
$0,6,\overline{11}$	1.86	< 3.4	+1.9
072	1.89	< 3.2	-1.2
$07\bar{1}$	1.85	< 3.5	-0.3
$07\bar{1}$	1.81	< 3.8	-0.5
$07\bar{2}$	1.80	< 3.8	-0.7
$07\bar{3}$	1.80	< 3.8	+0.9
$07\bar{4}$	1.80	< 3.8	-3.3
$07\bar{5}$	1.81	< 3.8	-2.7
$07\bar{6}$	1.83	< 3.6	+0.5
$07\bar{7}$	1.86	< 3.4	-0.4
$07\bar{8}$	1.90	< 3.1	-0.1

hkl	2sinθ	F meas.	F calc.
1,0,14	1.86	< 2.7	-0.7
1,0,13	1.73	< 3.4	+0.1
1,0,12	1.60	< 3.8	+2.4
1,0,11	1.48	12.4	-13.3
1,0,10	1.35	17.6	-14.6
109	1.23	< 3.8	+4.3
108	1.11	< 3.6	-0.7
107	0.98	5.3	-4.4
106	0.86	11.9	+11.4
105	0.74	21.2	+16.1
104	0.61	4.7	+3.9
103	0.50	6.7	-5.2
102	0.39	< 1.9	+3.3
101	0.29	< 1.6	+0.9
$10\bar{1}$	0.20	1.3	+1.1
$10\bar{2}$	0.26	2.1	-2.7
$10\bar{3}$	0.35	< 1.7	-2.3
$10\bar{4}$	0.46	< 2.0	+0.5
$10\bar{5}$	0.58	< 2.3	-1.7
$10\bar{6}$	0.70	3.7	+1.9
$10\bar{7}$	0.82	< 2.9	+0.5
$10\bar{8}$	0.95	< 3.2	-2.0
$10\bar{9}$	1.07	< 3.5	+2.5
$1,0,\overline{10}$	1.19	5.4	-3.5
$1,0,\overline{11}$	1.31	11.9	-9.9
$1,0,\overline{12}$	1.45	< 4.0	-1.9
$1,0,\overline{13}$	1.57	< 3.8	+1.9
$1,0,\overline{14}$	1.70	< 3.5	-0.8
$1,0,\overline{15}$	1.82	< 2.9	+0.5
2,0,13	1.84	< 2.8	-0.5
2,0,12	1.72	< 3.4	+0.8
2,0,11	1.60	< 3.8	-2.3
2,0,10	1.47	6.9	+5.2
209	1.35	< 4.0	-0.9
208	1.24	< 3.9	-1.3
207	1.12	< 3.6	-1.5
206	1.00	< 3.4	+0.4
205	0.88	24.8	+26.8
204	0.77	2.8	+0.8
203	0.66	4.2	-0.7
202	0.57	5.6	+4.9
201	0.49	12.5	-19.0

hkl	2sinθ	F meas.	F calc.	hkl	2sinθ	F meas.	F calc.
$20\bar{1}$	0.39	73.8	+86.3	$3,0,\bar{16}$	1.86	< 2.7	-0.3
$20\bar{2}$	0.40	22.9	-28.2				
$20\bar{3}$	0.44	12.4	+9.8	4,0,11	1.88	< 2.5	-0.1
$20\bar{4}$	0.51	4.7	-1.7	4,0,10	1.77	< 3.2	+3.5
$20\bar{5}$	0.61	< 2.4	-2.3	409	1.65	< 3.7	+0.1
$20\bar{6}$	0.71	18.3	+26.5	408	1.54	< 3.9	-0.4
$20\bar{7}$	0.82	4.1	-5.9	407	1.44	< 4.0	+0.5
$20\bar{8}$	0.92	< 3.1	+1.3	406	1.34	< 4.0	-2.0
$20\bar{9}$	1.04	< 3.5	-0.4	405	1.23	9.4	+11.0
$2,0,\bar{10}$	1.16	< 3.7	+0.1	404	1.13	11.6	+14.9
$2,0,\bar{11}$	1.28	7.9	+4.9	403	1.05	< 3.5	-5.3
$2,0,\bar{12}$	1.40	< 4.0	+1.6	402	0.97	< 3.3	+3.1
$2,0,\bar{13}$	1.52	< 4.0	+0.4	401	0.90	< 3.1	-2.4
$2,0,\bar{14}$	1.65	< 3.7	+3.0	$40\bar{1}$	0.80	< 2.9	+27.6
$2,0,\bar{15}$	1.77	< 3.1	-1.6	$40\bar{2}$	0.78	3.4	-2.5
				$40\bar{3}$	0.78	< 2.8	-2.5
3,0,12	1.85	< 2.8	-2.4	$40\bar{4}$	0.80	< 2.9	+3.7
3,0,11	1.73	3.4	-4.0	$40\bar{5}$	0.84	< 3.0	+2.1
3,0,10	1.61	11.9	-14.0	$40\bar{6}$	0.89	21.4	+21.4
309	1.50	< 4.0	-1.9	$40\bar{7}$	0.95	5.6	+9.5
308	1.38	< 4.0	+2.7	$40\bar{8}$	1.03	3.1	-5.1
307	1.27	< 3.9	-4.1	$40\bar{9}$	1.12	< 3.6	+4.7
306	1.16	< 3.7	+3.5	$4,0,\bar{10}$	1.21	< 3.8	-2.3
305	1.05	4.3	+9.8	$4,0,\bar{11}$	1.31	4.9	+2.5
304	0.95	< 3.2	+7.9	$4,0,\bar{12}$	1.41	3.7	+3.1
303	0.86	< 3.0	-3.2	$4,0,\bar{13}$	1.52	< 4.0	-0.5
302	0.77	< 2.8	-1.3	$4,0,\bar{14}$	1.63	< 3.7	+1.3
301	0.70	< 2.6	+1.9	$4,0,\bar{15}$	1.74	< 3.4	-3.0
$30\bar{1}$	0.60	< 2.3	+5.5	$4,0,\bar{16}$	1.86	< 2.7	+0.8
$30\bar{2}$	0.58	< 2.3	-0.9				
$30\bar{3}$	0.60	< 2.3	-3.3	509	1.83	< 2.9	-3.5
$30\bar{4}$	0.64	3.9	+6.2	508	1.72	< 3.4	+1.9
$30\bar{5}$	0.70	9.1	-7.3	507	1.62	< 3.8	+1.5
$30\bar{6}$	0.77	19.3	-16.9	506	1.52	< 4.0	+0.9
$30\bar{7}$	0.86	4.3	-7.1	505	1.42	5.7	+0.1
$30\bar{8}$	0.96	< 3.3	-4.1	504	1.33	6.3	-1.1
$30\bar{9}$	1.06	< 3.5	-0.8	503	1.25	< 3.9	-2.4
$3,0,\bar{10}$	1.17	< 3.8	+1.5	502	1.18	< 3.8	+1.2
$3,0,\bar{11}$	1.28	6.8	+7.5	501	1.12	< 3.6	+1.3
$3,0,\bar{12}$	1.39	< 4.0	+4.7	$50\bar{1}$	1.02	< 3.4	+1.9
$3,0,\bar{13}$	1.50	< 4.0	-0.5	$50\bar{2}$	0.98	< 3.3	+3.6
$3,0,\bar{14}$	1.62	< 3.8	+0.1	$50\bar{3}$	0.97	< 3.3	-4.0
$3,0,\bar{15}$	1.74	< 3.3	+0.1	$50\bar{4}$	0.98	< 3.3	+3.9

hkl	2sinθ	F meas.	F calc.
$50\bar{5}$	1.00	< 3.4	+0.6
$50\bar{6}$	1.03	3.4	-9.3
$50\bar{7}$	1.08	3.6	-9.4
$50\bar{8}$	1.14	< 3.7	-0.3
$50\bar{9}$	1.21	< 3.8	+3.7
$5,0,\bar{10}$	1.29	< 4.0	-4.9
$5,0,\bar{11}$	1.37	9.9	+7.4
$5,0,\bar{12}$	1.46	15.4	+16.8
$5,0,\bar{13}$	1.56	< 3.9	+2.0
$5,0,\bar{14}$	1.66	< 3.6	-1.7
$5,0,\bar{15}$	1.76	< 3.2	+1.1
5,0,$\bar{16}$	1.87	< 2.6	-0.7
607	1.80	< 3.0	+0.1
606	1.71	< 3.4	-0.7
605	1.62	< 3.8	+1.5
604	1.53	< 4.0	+7.3
603	1.46	< 4.0	+3.1
602	1.39	< 4.0	-3.0
601	1.33	< 4.0	+1.7
$60\bar{1}$	1.22	13.9	-8.2
$60\bar{2}$	1.19	8.5	-6.8
$60\bar{3}$	1.17	< 3.8	+0.3
$60\bar{4}$	1.17	< 3.8	+3.7
$60\bar{5}$	1.17	< 3.8	-4.5
$60\bar{6}$	1.19	10.7	+8.6
$60\bar{7}$	1.23	10.9	+13.2
$60\bar{8}$	1.28	< 3.9	-1.2
$60\bar{9}$	1.33	< 4.0	-1.9
$6,0,\bar{10}$	1.39	< 4.0	+0.7
$6,0,\bar{11}$	1.47	< 4.0	+0.1
$6,0,\bar{12}$	1.54	3.9	+4.8
$6,0,\bar{13}$	1.63	< 3.7	+0.9
$6,0,\bar{14}$	1.72	< 3.4	-0.7
$6,0,\bar{15}$	1.82	< 2.9	+0.3
705	1.82	< 2.9	+0.7
704	1.73	8.3	-5.7
703	1.66	< 3.6	-1.3
702	1.59	< 3.8	+0.4
701	1.53	< 4.0	-0.4
$70\bar{1}$	1.44	< 4.0	-0.3
$70\bar{2}$	1.40	< 4.0	+1.6
$70\bar{3}$	1.38	< 4.0	-0.4
$70\bar{4}$	1.36	< 4.0	+0.4
$70\bar{5}$	1.36	< 4.0	+0.7
$70\bar{6}$	1.37	< 4.0	-4.0
$70\bar{7}$	1.39	6.1	+1.6
$70\bar{8}$	1.43	< 4.0	+1.5
$70\bar{9}$	1.47	< 4.0	+1.3
$7,0,\bar{10}$	1.52	< 4.0	-0.4
$7,0,\bar{11}$	1.58	< 3.8	-1.2
$7,0,\bar{12}$	1.65	11.7	+12.4
$7,0,\bar{13}$	1.72	3.4	+7.2
$7,0,\bar{14}$	1.80	< 3.0	-2.5
$7,0,\bar{15}$	1.89	< 2.5	+0.7
802	1.81	< 3.0	-0.5
801	1.74	< 3.3	-1.9
$80\bar{1}$	1.64	7.9	-4.4
$80\bar{2}$	1.61	9.3	-7.6
$80\bar{3}$	1.58	< 3.8	-0.9
$80\bar{4}$	1.56	< 3.9	+2.0
$80\bar{5}$	1.56	< 3.9	-1.7
$80\bar{6}$	1.56	< 3.9	+1.1
$80\bar{7}$	1.57	< 3.9	+5.8
$80\bar{8}$	1.60	< 3.8	+1.7
$80\bar{9}$	1.63	< 3.8	-0.5
$8,0,\bar{10}$	1.67	< 3.6	+0.5
$8,0,\bar{11}$	1.72	< 3.4	-0.4
$8,0,\bar{12}$	1.78	< 3.1	+2.7
$8,0,\bar{13}$	1.84	< 2.8	+3.3
$90\bar{1}$	1.86	< 2.7	-0.3
$90\bar{2}$	1.82	< 3.0	-0.1
$90\bar{3}$	1.79	< 3.1	-0.8
$90\bar{4}$	1.77	< 3.2	+0.4
$90\bar{5}$	1.76	< 3.2	+0.1
$90\bar{6}$	1.75	< 3.3	-0.5
$90\bar{7}$	1.75	8.4	+5.6
$90\bar{8}$	1.77	< 3.2	+3.3
$90\bar{9}$	1.79	< 3.1	-1.5
$9,0,\bar{10}$	1.82	< 2.9	+0.1
$9,0,\bar{11}$	1.87	< 2.6	-1.2

REFERENCES.

1. Booth, A. D. (1946) Proc. Roy. Soc., A183, 388.
2. Booth, A. D. (1948) "Fourier Technique in X-ray Organic Structures", Cambridge University Press.
3. Bowen, E. J. (1945) J. Chem. Phys., 13, 306.
4. Bowen, E. J. and Mikiewicz, E. (1947) Nature 159, 706.
5. Bradley, A. J. and Jay, A. H. (1932) Proc. Phys. Soc., 44, 563.
6. Bragg, W. H. (1921) Proc. Roy. Soc., 34, 33.
7. Brockway, L. O, and Robertson, J. M. (1939) J. Chem. Soc., 1324.
8. Clar, E. (1932) Ber., 65, 503.
9. Clar, E. (1942) Ber., 75, 1271.
10. Coulson, C. A. (1939) Proc. Roy. Soc., A 169, 413.
11. Coulson, C. A. (1941) Proc. Roy. Soc. Edin., 61, 115.
12. Coulson, C. A. and Daudel, P. and R. (1947) Rev. Sci.
13. Cox, E. G. and Shaw, W. F. B. (1930) Proc. Roy. Soc., A 127, 71.
14. Daudel, R. and Pullman, A. (1945) Compt. Rend., 220, 888.
15. Daudel, P. and R. (1948) J. Chem. Phys., 16, 639.
16. Daudel, R. (1949) Private Communication.
17. Forster, Th. (1938) Z. Phys. Chem., B 41, 287.
18. Ganguly, S. C. (1945) J. Chem. Phys., 13, 128.

19. Gaubert, P. (1905) Bull. Soc. franc. mineral., 28, 286.

20. Gold, V. (1949) Trans. Farad. Soc., 45, 2, 191.

21. Hertel, E. and Bergk, H. W. (1936) Z. Phys. Chem., 33, 319.

22. Huckel, E. (1931) Z. Physik., 70, 204.

23. Jeffrey, G. A. (1945) Proc. Roy. Soc., A 183, 388.

24. Jonnson, C. V. (1941) Ark. Kem. Min. Geol., 15 A, 14, 1.

25. Krishnan, K. S. and Seshan, P. K. (1934) Z. Krist., A 89, 538.

26. Lennard-Jones, J. E. and Coulson, C. A. (1939) Trans. Farad. Soc., 352, 811.

27. Pauling, L. and Wheland, G. W. (1933) J. Chem. Phys., 1, 362.

28. Pauling, L., Brockway, L. O. and Beach, J. Y. (1935) J. Amer. Chem. Soc., 57, 2705.

29. Pauling, L. and Brockway, L. O. (1937) J. Amer. Chem. Soc., 59, 1223.

30. Pauling, L. (1942) "The Nature of the Chemical Bond", Cornell University Press.

31. Penney, G. W. (1937) Proc. Roy. Soc., A 158, 306.

32. Robertson, J. M. (1933) Proc. Roy. Soc., A 140, 79.

33. Robertson, J. M. (1943) J. Sci. Instr., 20, 175.

34. Robertson, J. M. and White, J. G. (1945) J. Chem. Soc., 607.

35. Robertson, J. M. and White, J. G. (1947) J. Chem. Soc., 358.

36. Robertson, J. M. and White, J. G. (1947) J. Chem. Soc., 1001.

37. Robertson, J. M. (1948) J. Sci. Instr., 25, 28.

38. Scheibe, G., Muller, R. and Schiffmann, R. (1941) Z. Phys. Chem., B 49, 324.

39. Seshan, P. K. (1936) Proc. Indian Acad. Sci., 2, 148.

40. Sherman, J. (1934) J. Chem. Phys., 2, 488.

41. Siegbahn, M. (1931) "Spektroscopie der Rontgenstrahlen".

42. Svartholm, N. (1941) Ark. Kem. Min. Geol., 15 A, 13, 1.

43. Tunell, G. (1939) Amer. Min., 24, 448.

44. White, J. G. (1948) J. Chem. Soc., 1398.

45. Wilson, A. J. C. and Lipson, H. (1941) Proc. Phys. Soc., 53, 245.